STRUCTURAL SAFETY OF BRIDGE DECKS WITH VARIABLE REBAR COVER

by

PREM VASANT EGADE

Presented to the Faculty of the Graduate School of

The University of Texas at Arlington in Partial Fulfillment

of the Requirements

for the Degree of

MASTER OF SCIENCE IN STRUCTURES AND APPLIED MECHANICS

THE UNIVERSITY OF TEXAS AT ARLINGTON

December 2018

Acknowledgements

Firstly, I would like to express my sincere gratitude to my advising Prof. Nur Yazdani who provided me the resources and guidance to complete this thesis. His guidance helped me in all phases of research and writing of this thesis.

Besides my advisor, I would like to thank the rest of my committee: Prof. Himan Hojat Jalali and Prof. Samantha Sabatino for their encouragement and suggestions. My sincere thanks also go to Dr. Eyosias Beneberu and Towfiqul Quadir for sharing their experience and knowledge.

Finally, I would like to thank all the friends from The University of Texas at Arlington for providing me with a happy environment and make me feel like home.

November 26, 2018

Abstract

STRUCTURAL SAFETY OF BRIDGE DECKS

WITH VARIABLE REBAR COVER

Prem V. Egade, MS

The University of Texas at Arlington, 2018

Supervising Professor: Nur Yazdani

Construction defects are common and are difficult to avoid completely. This arises due to improper workmanship, inspection, drawing and specification. On bridge decks, achieving the desired cover is necessary since inadequacy can cause accelerated corrosion in steel and for the most part spalling and delamination which ultimately led to failure. Tolerance provided by different standards and specification also restrict the amount of rebar. So, construction is more focused on increasing cover undermining the loss of strength as consequence. The objective of this research is to check the safety of decks by analyzing bridges for reduction in capacity due to cover variation.

The investigation was conducted on two old and two new bridges using Ground Penetration Radar (GPR) for possible rebar cover variation. Data were collected with ground coupled high-frequency 2.6GHz antenna for high accuracy. The dielectric constant for depth calculation was estimated using migration and ground truth method with minimum error. The hyperbolic signatures were detected and plotted in form of contours and percent distribution was calculated.

For 0.5 in. (13mm) and 1 in. (25.4mm) increase in rebar cover, the deck capacity is reduced by 9% and 18%, respectively for 8.5 in. (216mm) thickness of the slab. It was found that on average the rebar cover distribution of 40% and 77% varied +1/2 inch and

+1 inch, respectively. The reduced negative moment capacity followed by decreased effective depth is compared with design moments. Finally, the load on rebar cage is modeled and deflection and stresses are calculated different bar sizes and distance of rebar supports. The smaller size rebar with less spacing deflected more than larger size rebars.

Table of Contents

List of Illustrations

List of Tables

Chapter 1

Introduction

1.1 Introduction

Construction defects are common and are difficult to avoid completely. Some of the causes are improper workmanship, lack of inspection, not following specifications, unskilled labor, incomplete design drawings and lack of knowledge. Due to this performance of the structures, cost of maintenance or repair are severely affected. One such defect is proper placement of rebars in the concrete member which helps achieve desired resistance against applied loads.

The cover is also necessary to assure enough bond strength along with this positioning is also significant, lowering the top bars or raising the bottom bars by ½ inch more than that specified in a 6-inch-deep slab could reduce its load-carrying capacity by 20% (concreteconstruction.net, 2005). During construction, rebar may displace vertically due to insufficient support and will result to loss in capacity.

GPR has been successfully used in the measurement of rebar depth, asphalt, concrete deck pavement, base and sub-base with high accuracy (Al-Qadi & Samer, 2005). Earlier it was used to achieve qualitative data now with progressive research and development of different systems quantitative data can be gathered. It has been effectively used for mapping concrete deterioration (Parrillo & Roberts, 1997) and corrosion in rebar (Hasan, Quantitative Non-destructive Evaluation Of Rebar Diameter And Corrosion Damage In Concrete Using Ground Penetrating Radar, 2015) has aided to predict maintenance required.

1.2 Problem Statement

Errors are common in construction of reinforced concrete structures. Incomplete drawing details, improper execution, bad inspection practices, lack of knowledge and

experience will cause error in construction. The impact is on cost, time, loss of lives and credibility. The Study was conducted by Multidisciplinary Center for Earthquake Engineering Research (MCEER) on 1062 bridges in United States between 1980-2012. Causes of failure due to environmental, earthquake, collision, scour, flood, fire, wind, overload and internal causes were reported. The flood (28%), scour (19%) and collision (15%) were at top but internal causes (11%) were close at fifth position. Internal cause includes design error, material defects and deficiency in construction.

Maintaining uniform rebar clear cover is one of the challenges of bridge deck construction. Since, corrosion is the single most important factor that governs the service life of the deck. Hence, adequate cover is provided to ensure that rebar stays intact from the salts and water. Tolerance are strict against providing cover less than specified this has led contractors to implement increased rebar cover sacrificing flexural resistance.

1.3 Objective

- Analyzing the cover variation in concrete bridge deck.
- Calculation of reduced capacity of deck due to insufficient cover.
- Comparing capacity with design moment from dead and live load.
- Testing out the use of different bar sizes in concrete deck construction.
- Effect of less spacers(supports) in rebar cage construction.

1.4 Organization of study

Chapter 1 gives introduction to problem and outlines the objectives.

Chapter 2 starts with brief introduction of cover for reinforcement on bridge deck. GPR working and theory and governing factor for depth measurement are explained. Previous research on defects and corresponding finding are listed out.

Chapter 3 is the description of the bridges investigated for rebar cover variation.

Chapter 4 describes the process of data collection, post-processing and plotting contours.

Chapter 5 deals with calculation of negative flexural resistance and design negative moments.

Chapter 6 is results and discussions of contours along with rebar distribution, comparative study between capacity and design moments. Analysis of a major cause of deflection in rebar

Chapter 7 conclusions are stated for this study and future work is suggested

Chapter 2

Literature Review

2.1 Concrete Cover

The distance from the surface of embedded steel in concrete to the outer surface of the concrete is termed as clear cover. It protects rebar against the outside environment responsible for corrosion, distribute stress in concrete, responsible for bond strength and provide thermal insulation. The thickness of the cover is mostly depended on the type of structural element and environmental condition. On bridge deck, top of the concrete slab is subjected to abrasion from vehicle, water and deicing salts hence provided more as compared to bottom cover where no such forces exist. The effective cover is measured from the center of rebar while clear cover from the outer surface. Figure 2-1 shows the cover in deck for top reinforcement and bottom.

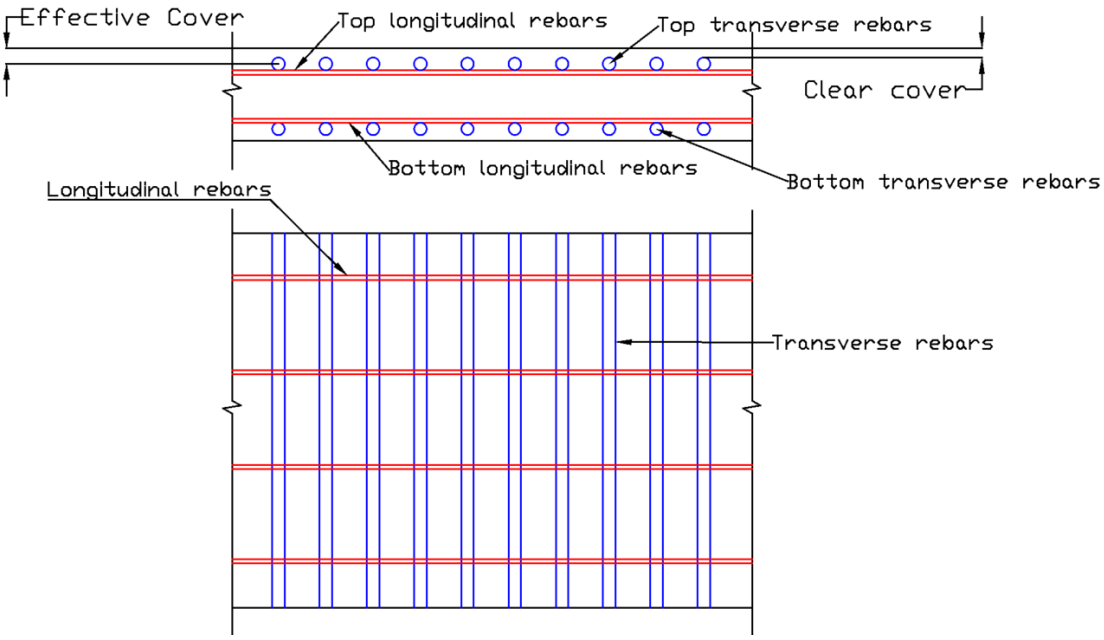

Figure 2-1 Cover on deck for top reinforcement

American Association of State Highway and Transportation Officials (AASTHO, 2017) suggest 1 in. (25mm). as minimum cover to be provided to main reinforcement (included epoxy coated). Cover for unprotected reinforcing steel shall be less than that specified in Figure 2-2 (Table 5.10.1-1) (AASHTO, 2017). High cover is recommended for corrosive environment such as direct exposure to salt water and earth. Some owner has cover requirement more that values listed in Table 5.10.1-1. Texas Department of Transportation (TxDOT) Standard Specifications for Construction and Maintenance of Highways, Streets, and Bridges also specify minimum cover of 1 in. (25mm) if not specified.

Situation	Cover (in.)
Direct exposure to salt water	4.0
Cast against earth	3.0
Coastal	3.0
Exposure to deicing salts	2.5
Deck surfaces subject to tire stud or chain wear	2.5
Exterior other than above	2.0
Interior other than above • Up to No. 11 bar • No. 14 and No. 18 bars	 1.5 2.0
Bottom of cast-in-place slabs • Up to No. 11 bar • No. 14 and No. 18 bars	 1.0 2.0
Precast soffit form panels	0.8
Precast reinforced piles • Noncorrosive environments • Corrosive environments	 2.0 3.0
Precast prestressed piles	2.0
Cast-in-place piles • Noncorrosive environments • Corrosive environments o General o Protected • Shells • Auger-cast, tremie concrete, or slurry construction	 2.0 3.0 3.0 2.0 3.0
Precast concrete box culverts • Top slabs used as a driving surface • Top slabs with less than 2.0 ft of fill not used as a driving surface • All other members	 2.5 2.0 1.0

Figure 2-2 Table 5.10.1-1 (AASHTO, 2017)

2.2 Introduction of GPR

GPR is a non-destructive method which uses electromagnetic waves for subsurface imaging. It comes with various sizes and the wide range of antenna frequency which enables to produce images of a target with different size, shape, material and at greater depth. It has found its usefulness in utility detection, archaeological, environmental, concrete assessment, search and rescue operation, geotechnical and geological fields. With the advancement of the system, post-processing techniques, research and operating practices.

GPR system consists of a control unit, power supply, and antenna. Control unit has electronics which trigger electromagnetic pulse. Antenna housing contains transmitter and receiver, transmitting and receiving reflected energy from objects buried, respectively. When this radar energy encounters a difference in medium three things happen, part of it penetrates, reflects and absorb by the surface. Figure 2-3 shows the Transmitter (Tx) emitting radar energy (red wave) into subsurface material 1. After reaching the interface of two material part of the energy is reflected and captured by Receiver (Rx), part of it is refracted and enter medium 2. This process continues till the radar energy is attenuated. Analyzing the reflected waves gives useful information about subsurface material properties.

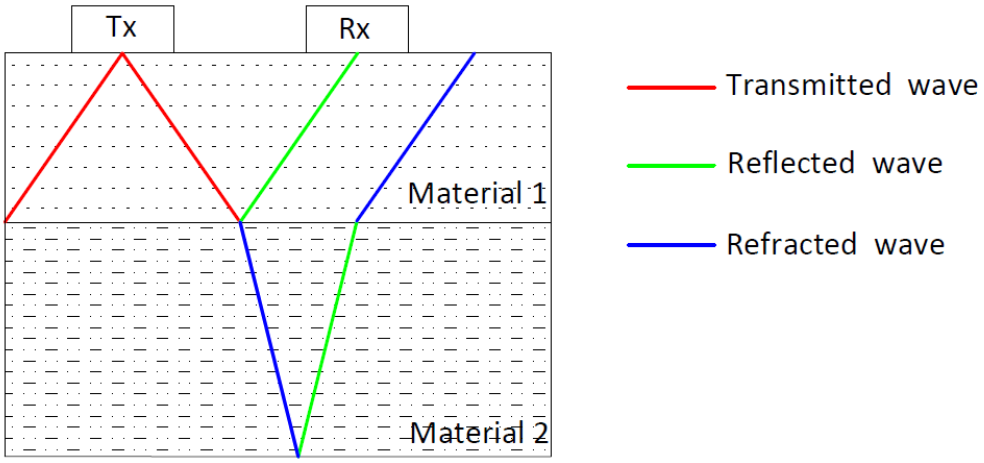

Figure 2-3 Radar waves in different medium

Material Properties

The radar energy response is governed by two physical properties of medium electrical conductivity and dielectric constant. The absorption may be high or low depending on the electrical conductivity. For low conductive material like dry concrete or soil, the waves penetrate deeper. On the other hand, if it's high for example fresh concrete or metal the GPR energy is attenuated before it travels greater depth. The dielectric constant controls the velocity of radar waves traveling through the medium and is given by Equation 2-1.

$$\nu = \frac{c}{\sqrt{\varepsilon}}$$

Equation 2-1, (Geophysical Archaeometry Laboratory Inc., 2018)

Where, ν = velocity of radar wave in medium (x10^9 m/s)

c = velocity of light in vacuum, 0.3x10^9 m/s

ε = relative permittivity of medium

The velocity of waves is inversely proportional to the square root of the dielectric constant of a medium. So, if it's lower the waves travel at a high velocity and vice versa. It is an important property in depth detection of any buried objects. Most of the construction material it varies from 3 to 12. Some common dielectric constants are tabulated in Table 2-1. Accurately identification will reduce error in determining the depth of an object.

Table 2-1 Dielectric Constant of Different Materials

Materials	**Dielectric Constant**	**Materials**	**Dielectric Constant**
Air	1	Granite (dry)	5-8
Clay (dry)	2-20	Granite (wet)	5-15
clay (wet)	15-40	Limestone (dry)	4-8
Concrete (dry)	4-10	Limestone (wet)	6-15
Concrete (wet)	10-20	Sand (dry)	4-6
Asphalt	5	Sand (wet)	10-30
Fresh Water	81	Soil (average)	16
Fresh water ice	3-4	Iron Oxides	14

When radar wave enters a different medium, the contrast in the reflection in the image is directly proportional to the difference in the dielectric constant of materials. For example, the concrete-asphalt interface causes less contrast than the concrete-metal. The strength of contrast is tabulated Table 2-2 for different material interface.

Table 2-2 Reflection Strength at Boundary of Two Materials

Boundary	**Dielectric Contrast**	**Reflection Strength**
Asphalt - Concrete	Medium	Medium
Concrete - Sand	Low	Weak
Concrete - Air	High, phase reversal	Strong

Concrete Deck - Concrete Beam	None	No reflection
Concrete - Metal	High	Strong
Concrete - Water	High	Strong
Concrete - PVC	Low to Medium, phase reversal	Weak

Antenna and T-R offset

There are various frequency antennas available ranging from 10Mhz to 2600MHz. Lower frequency antenna (10Mhz to 900Mhz) penetrates higher depth, suitable for utility locating, geological, environmental and archaeological purposes. They have the longer wavelength that cannot detect the smaller size targets. The high-frequency antennas (1000Mhz-2600Mhz) are used in concrete mapping, rebar and asphalt thickness measurement. This facilitates detection of smaller size objects since it has a shorter wavelength but with less penetration depth.

Generally, there is fix separation between transmitter and receiver. This helps in generating hyperbolas to measure velocity of materials accurately and eliminated surface reflection of waves before the ground (Geophysical Archaeometry Laboratory Inc., 2018). The Figure 2-4 shows the transmitting and receiving antenna separated by the distance TxxR.

Where,

T= two-way travel time;

V=wave velocity;

r= radius of the object;

x=horizontal separation;

d=depth of the object;

TxxR= transmitter-receiver separation

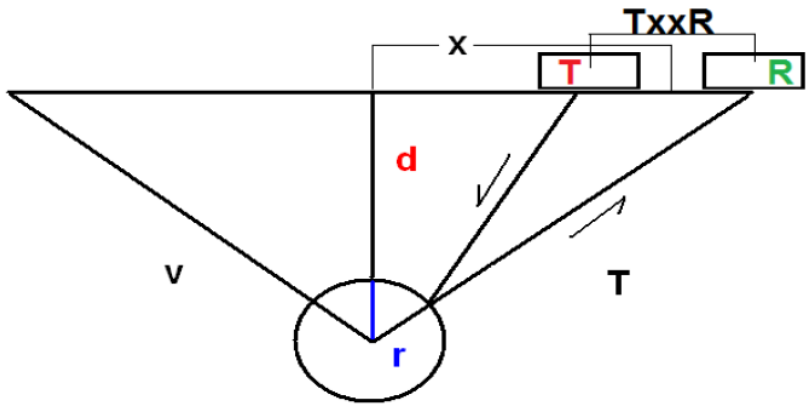

Figure 2-4 Separation between transmitter and receiver (Geophysical Archaeometry Laboratory Inc., 2018)

Working of GPR and Formation of Radargram

Radargram is the term used for output image generated by GPR. The antenna radiates energy in a wide cone. While scanning on a concrete deck with rebar, the reflection looks like the inverted hyperbola because the reflection is received by the receiver before the antenna is at top of rebar. The peak of the hyperbola in radargram represent the exact location of rebar. In Figure 2-5 when the antenna is at 1 the reflected wave is captured, and a point A is obtained in radargram. In a similar way when antenna moves from 1 to 5 it emits waves which get reflected by rebar and hyperbola is produced.

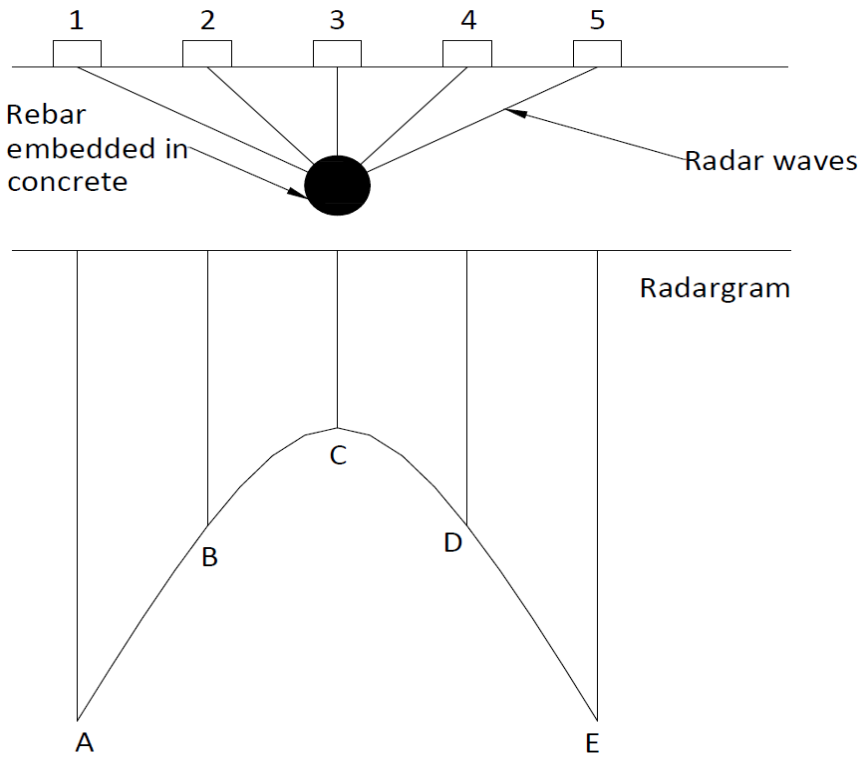

Figure 2-5 Formation of Radargram

When scanning on bridge deck rebars located at certain spacing produces series of hyperbola in radargram as shown in Figure 2-6.

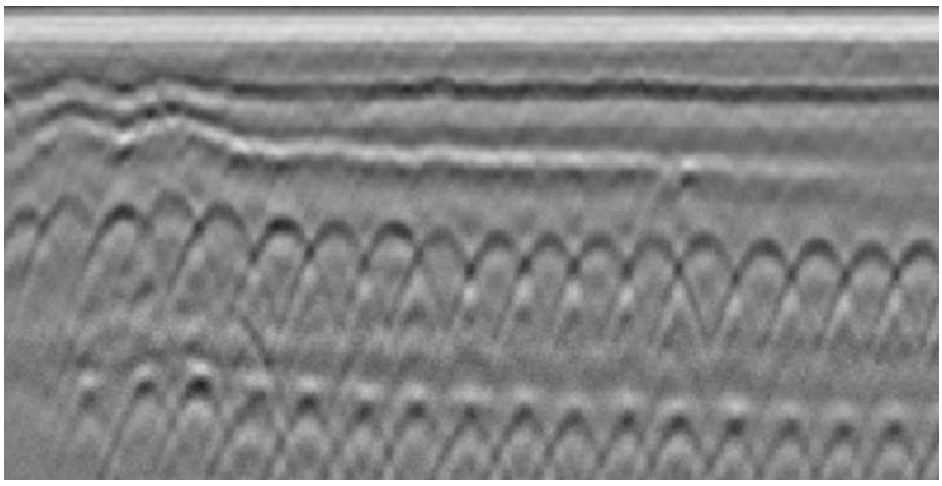

Figure 2-6 Typical Radargram of Bridges Deck

Scanning

The antenna can be held normal or cross-polarized (Figure 2-7). The line joining transmitter and receiver is perpendicular and parallel for normal or cross-polarized, respectively. The metal in concrete is more sensitive when scanned perpendicular to target and antenna held in a normal-polarized way. This is opposite when scanning over non-metallic targets.

Figure 2-7 Normal vs cross polarized (Geophysical Survey System, 2017)

The scans are represented as one(A-scans), two(B-scans) and three(C-scans) dimensions. When antenna transmitter and receiver is kept stationary and the image at that point is A-scan(Figure 2-8). The first wave indicates the top surface called direct coupling. When series of A-scans are collected with respect to time or distance covered while the antenna is dragged the images is called B-scans(Figure 2-8). C-scans are the collection of B-scans combined to which gives a three-dimensional image(Figure 2-9).

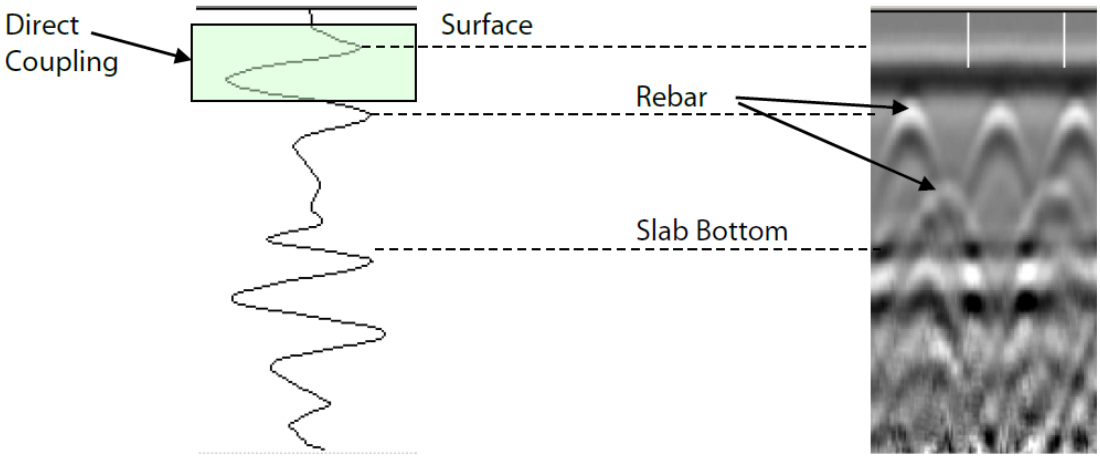

Figure 2-8 A-scan(left) and B-Scan(right), (Geophysical Survey System, 2017)

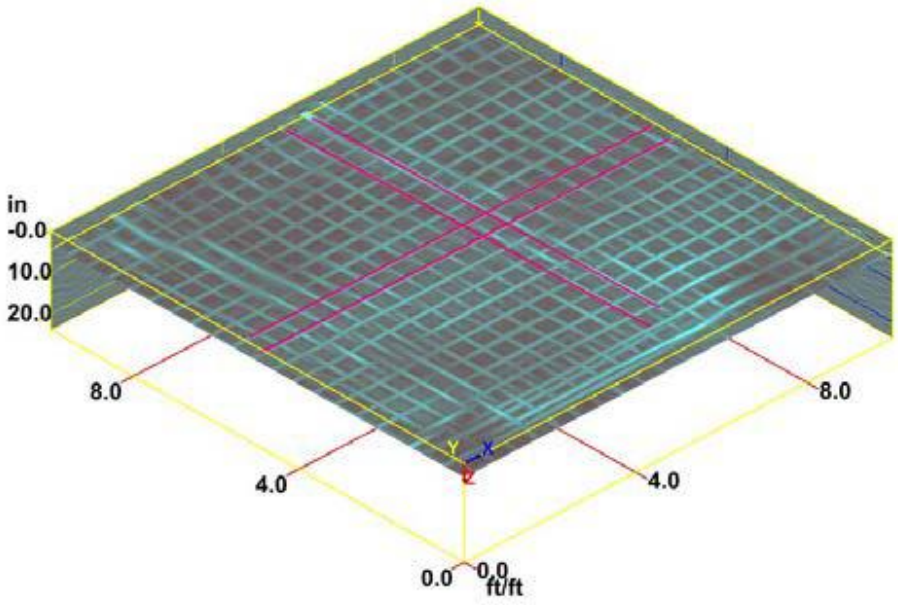

Figure 2-9 C-scan (Geophysical Survey System, 2017)

2.3 Previous Research

Hasan and Yazdani (2014) investigated rebar cover variation of concrete bridge deck near Roanoke, Texas using 2.6 GHz antenna. After applying time-zero correction and noise removal filter rebar hyperbolic signatures were picked using RADAN software provided by GSSI. The dielectric constant was found with a standard deviation of 1.29 and 2.89 from migration and ground truth method, respectively. This was accepted by keeping error percent below 15%. Cover at some region was inaccurately estimated due to the presence of water for curing. Rebar location and depth were plotted in form of contours which showed variation within range 1 to 4 in. (25.4 to 101.6 mm). It concluded less than 48% of the area of bridge deck had an inadequate cover, less than AASTHO specified minimum value of 2.5 in. (64mm). Span 3 (Figure 2-10) indicates most cover within range 2.5 to 3 in. (64 to 76 mm) colored as green and span 4 (Figure 2-11) indicates less cover within range 1 to 2 in. (25 to 51 mm) marked with warmer color.

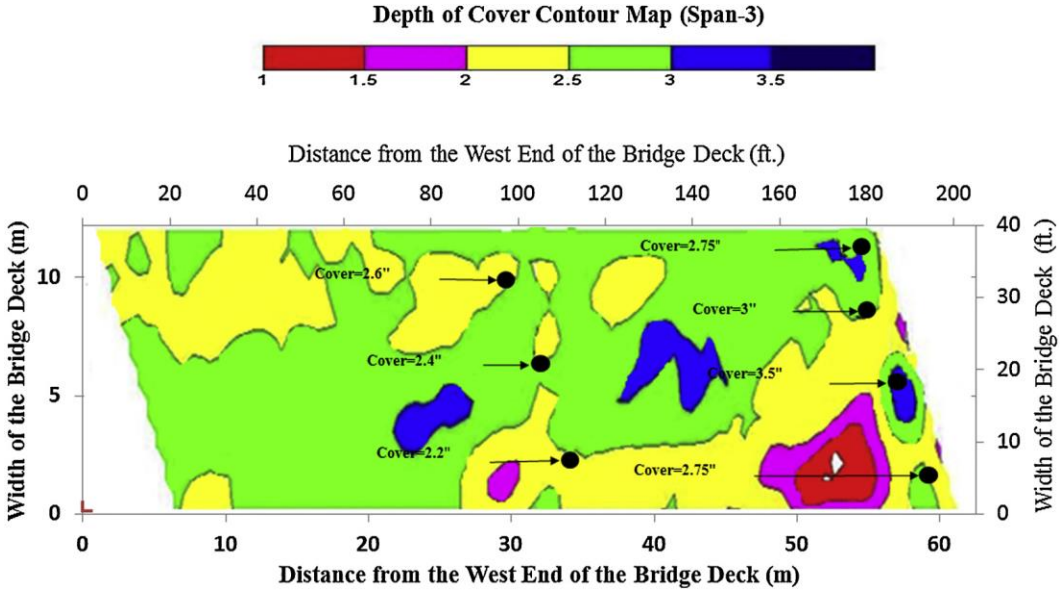

Figure 2-10 Variation of cover on span 3 (Hasan & Yazdani, 2014)

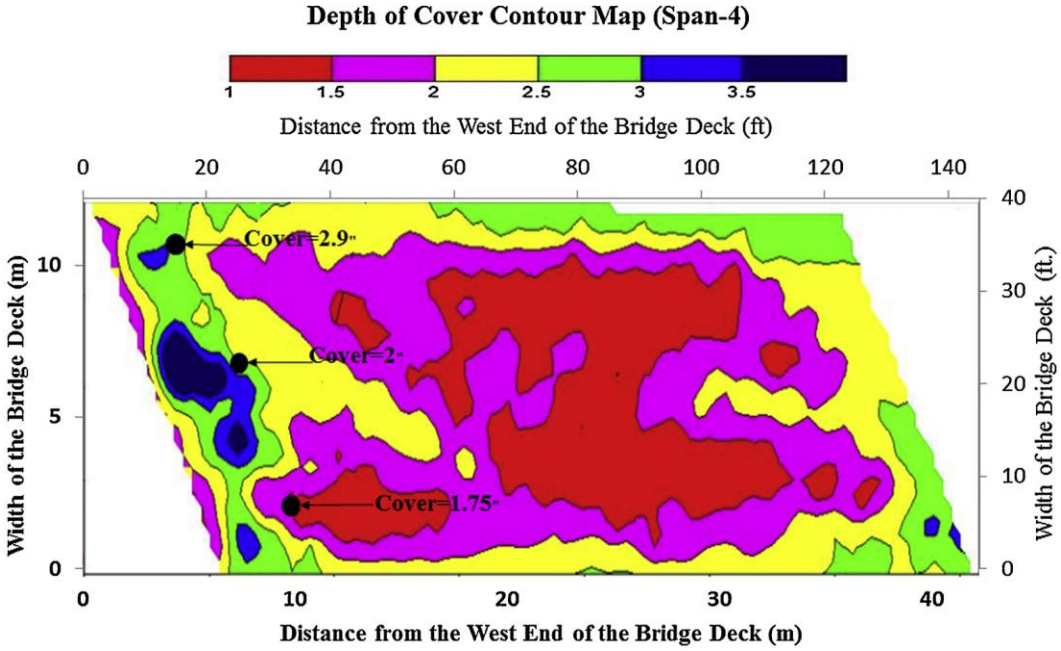

Figure 2-11 Variation of cover on span 4 (Hasan & Yazdani, 2014)

In the study Hugenschmidt, 2002 horn antenna(ground coupled) with a center frequency 1.2Ghz. A constant signal velocity of 0.9*108 m/s within the concrete was used to convert the original time axis to depth. A comparison between radar results and 15 cores resulted in a mean difference of 0.24 in. (6 mm) for 4 bridges. Figure 2-12 shows asphalt (gray arrow), white arrow (rebar) and black arrow (concrete bottom). The variation was seen in asphalt pavement thickness and rebar cover. The rapid measurement of thickness from GPR for was demonstrated.

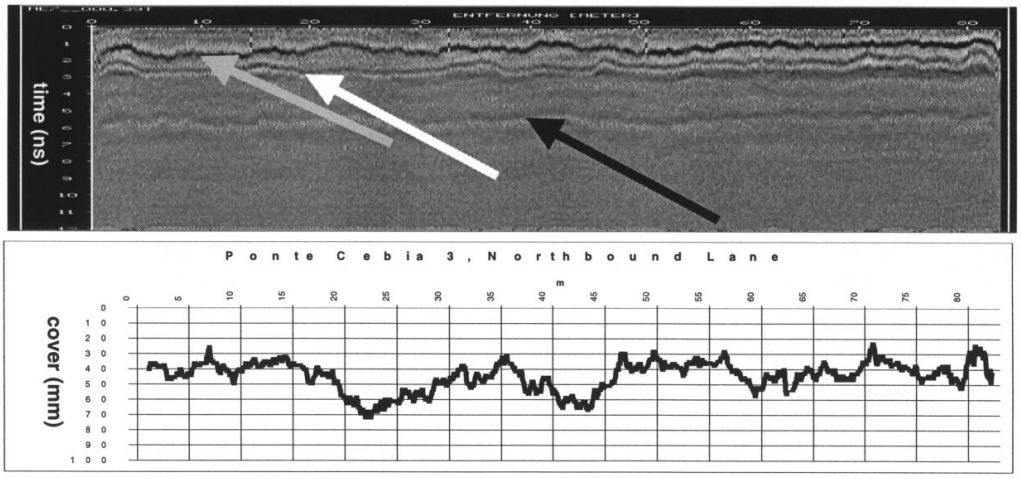

Figure 2-12 Variation in Asphalt Layer (gray arrow), Rebar (white arrow) and Concrete Bottom (black arrow), (Hugenschmidt, 2002)

The case study by Erdem and Peraza (2015) involved assessment of reinforced concrete wall defects. The building was for federal agency, so it was not subjected to local building code regulation and special inspection during construction. This building was constructed using insulated concrete forms which remains and serves a purpose of thermal insulation. The reinforcement location was not in accordance to design was found accidentally and honey combing at several location was observed. Detail inspection at 26 locations was carried using GPR to identify other construction defeats. The vertical reinforcing bars planned centered along the thickness of wall varied as much as ± 2¾ in. (69.85mm) beyond the tolerances ± 3/8 in. (9.525mm) provided by ACI. This was found in 12 of 26 located surveyed causing losses in strength for negative and positive bending. Figure 2-13 is the exposed reinforcement resulted with corresponding reduction of strength tabulated in Table 2-3. This indicated inspection before placement of concrete was not performed properly.

Figure 2-13 Exposed reinforcement in wall outline in red

Table 2-3: Reduction in Strength Due to Displaced Rebars (Erdem & Peraza, 2015)

Bar Position	**Strength ΦMn (kip-ft/ft)**	**Reduction %**
Center	2.96 (4.45kNm/m)	None
3/8” (9.525mm) off center	2.57 (11.44kNm/m)	13%
1.0” (25.4mm) off center	1.91 (8.5kNm/m)	35%
1.5” (38.1mm) off center	1.39 (6.19kNm/m)	53%
2.0” (50.8mm) off center	0.82 (3.65kNm/m)	72%
2.5” (63.5mm) off center	0.25 (1.12kNm/m)	92%

Based on #5 bar @16”, Grade 60 steel, 6” thick wall, 4,000 psi concrete

One of the most import aspect of constructions work is quality control which ensures execution according to design drawing and specifications. Ekolu and Solomon 2006 conducted statistical analysis of concrete cover in three newly constructed highway bridges. In this research, cover survey was conducted on deck, pier and abutment. The table summarizes the findings. The cover depth for soffit of deck was proposed 1.58 in. (40mm) and average was found higher of 1.97 in. (50mm), exceeding minimum cover. Some section had low cover while some had high cover. The consistent standard deviation of 0.28 was seen by deck and lower for piers of 0.2. While abutment showed higher standard deviation of 0.4. This concluded that the deck and piers were built with more controlled than abutment. Unlike piers and abutment, lowering of deck cover was suspected due to additional flexural action which tend to deflect rebars during compaction and concrete placement

Table 2-4: Summary of Rebar Cover Variation (Ekolu and Solomon 2006)

Bridge	Element	No. of data points	Average cover(in)	Standard deviation
Bridge 1	Deck	74	1.93 (49mm)	0.3
	Piers	11	1.97 (50mm)	0.2
	Abutments	26	1.97 (50mm)	0.59
	All elements	111	1.97 (50mm)	0.35
Bridge 2	Deck	78	1.81 (46mm)	0.27
	Piers	11	2.44 (62mm)	0.72
	Abutments	18	2.17 (55mm)	0.39
	All elements	107	2.13 (54mm)	0.43
Bridge 3	Deck	54	1.85 (47mm)	0.28
	Piers	20	1.93 (49mm)	0.19
	Abutments	36	2.17 (55mm)	0.45
	All elements	110	1.97 (50mm)	0.28

Chapter 3

Bridges Description

3.1 SH183 Over Loop 12

The Loop 12 bridge carrying State Highway 183 (SH 183) over Loop 12 was constructed in 1959 and later widened in 1969. It was a four span simply supported bridge. Its superstructure comprised pre-stressed concrete I-girder and composite cast-in-place concrete deck. There was impact damaged in 2006 (Figure 3-1) resulting in the replacement of a section of the third span superstructure. Figure 3-2 is the plan of bridge with different construction time and location of repaired deck. The location of bridge is shown in Figure 3-9 in red marker.

Figure 3-1 Impact Damage on Old SH183 over Loop 12

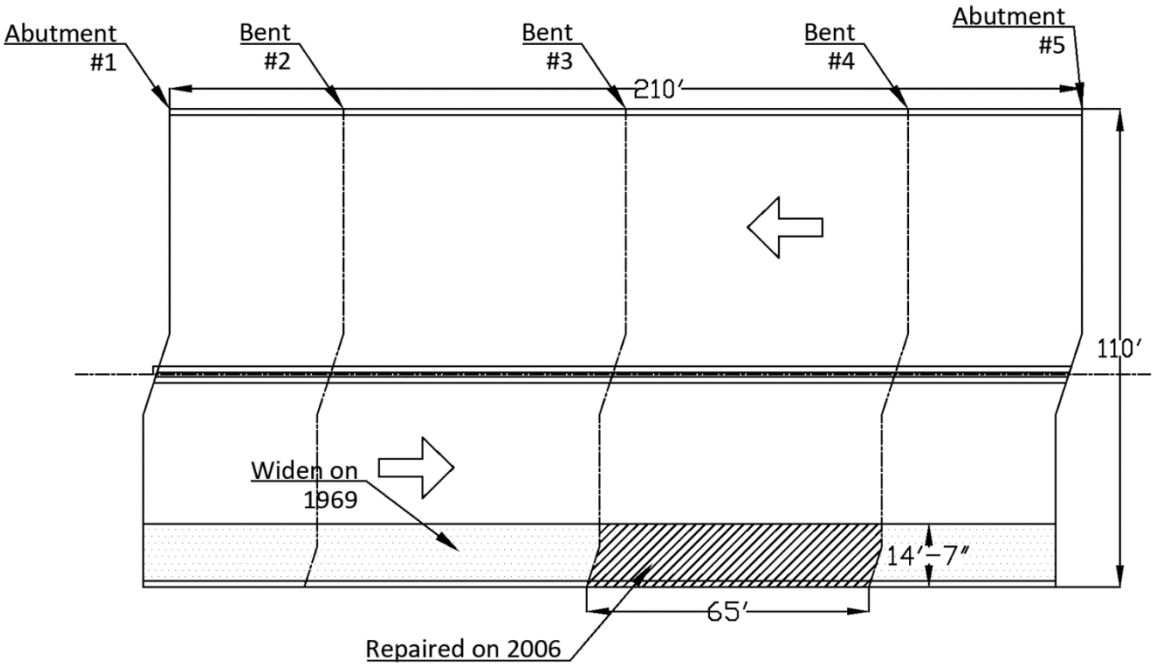

Figure 3-2 Time of Construction

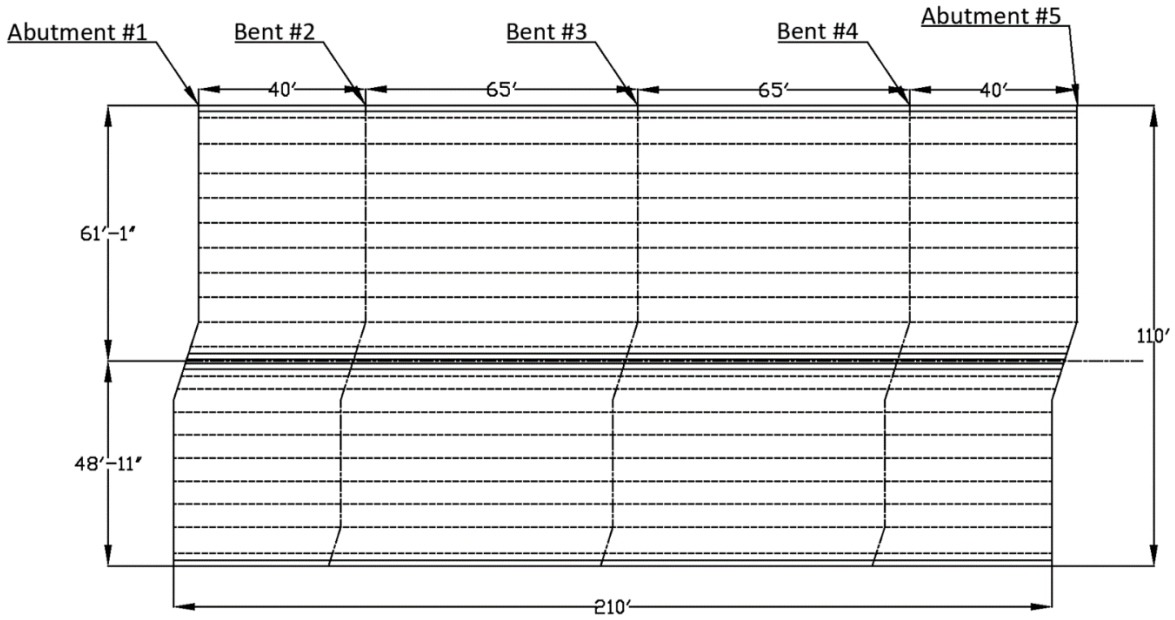

Figure 3-3 Layout of Old SH183 Over loop 12

The bridge was demolished and replaced in 2018 by two spans prestressed concrete bridge, SH183 General Purpose Lane(GPL) west bound (Figure 3-4) and (Managed Lane)ML over Loop 12 (Figure 3-5). The deck is continuous with precast panel with Class 'S' high performance concrete with f'c=4000 psi (27.58 N/mm^2).

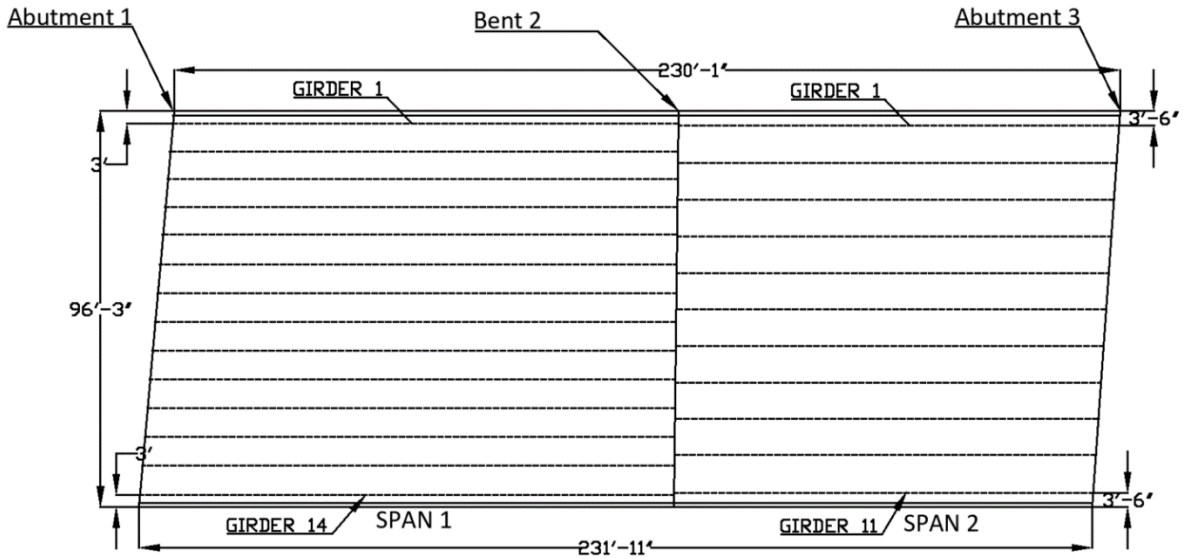

Figure 3-4 Layout of New SH183 GPL Over Loop 12(Westbound)

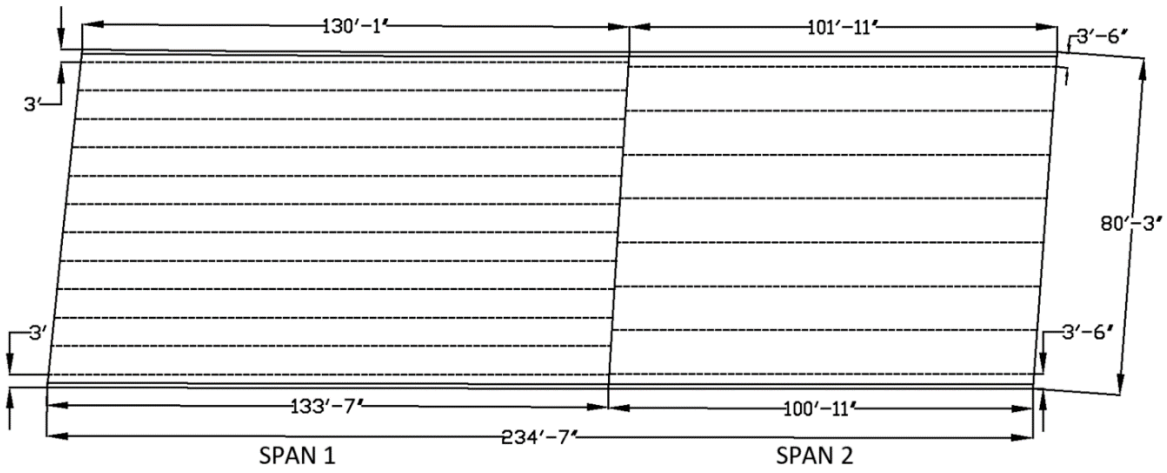

Figure 3-5 Layout of New SH183 ML Over Loop 12(Eastbound)

3.2 SH183 Over MacArthur Blvd

The old MacArthur Blvd Bridge carrying state highway 183 (SH 183) was constructed in 1958 and later widened in 1970. This bridge is cast-in place reinforced concrete with a continuous span and composite T-beam (Figure 3-7). On the morning of May 28, 2005, a fuel tanker carrying 300 gallons (1136 liter) of fuel heading east on SH 183 fell off the bridge and caught on fire below the bridge (Figure 3-6). The concrete in the bridge beams, columns and the deck suffered spalling and popping damage because of sustained fire. The damaged components were repaired using the mortar and strengthened with CFRP laminates.

Figure 3-6 Fire Damage on Old SH183 over MacArthur

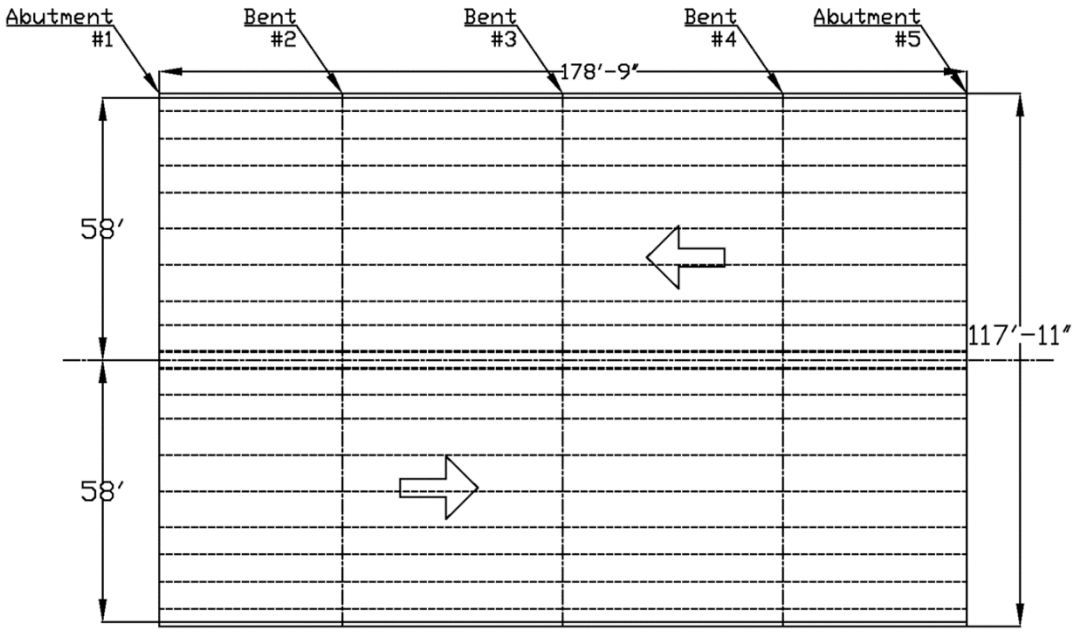

Figure 3-7 Layout of Old SH183 Over MacArthur

The bridge was demolished and replaced in 2018 by three spans prestressed concrete bridge (Figure 3-8). The location of bridge is shown in (Figure 3-9) in blue

marker. The deck is constructed continuous using precast panel with Class ‘S’ high performance concrete with f’c=4000 psi (27.58 N/mm^2).

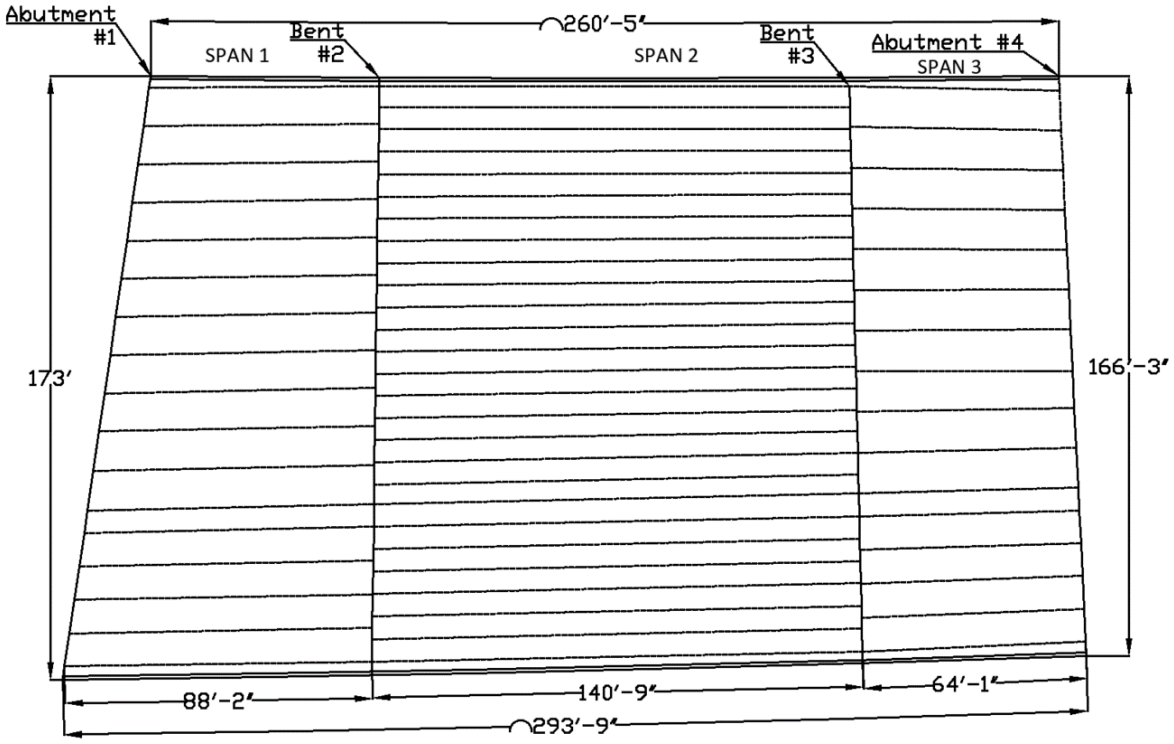

Figure 3-8 Layout of New SH183 Over MacArthur

Figure 3-9 Location of SH183 Over Loop 12 (red marker) and MacArthur (blue marker), (Google maps)

Chapter 4

Methodology

4.1 Data Collection

In this project, GPR used is SIR 30 from Geophysical Survey System, Inc and model 52000S with center frequency 2600Mhz. This gives depth range of 0 to 12 in. (0 to 305mm) ideal for structural element assessment. The range is depended on the conductance of concrete. So fresh or newer concrete being more conductive due to the presence of water waves will attenuate faster resulting in shallow penetration. This penetration range is enough to capture the top reinforcement in concrete deck and high frequency also help in generation high-resolution scans. The hand driven tri-wheel cart used for data collection shown Figure 4-1. The antenna was placed inside the cart such that it remains less than 1/2 in. (13mm) to surface throughout the scanning operation. If the antenna is not close to the surface it will result in loss of radar energy off the surface rather than penetrate through it.

Before data is collected using GPR the site is prepared. Bridge is closed for traffic by part or whole. The guidelines from start to end of bridge are marked at 3 feet spacing in transverse direction. First line 3 feet from rail to accommodate cart width. The purpose of this lines were to help to ensure the cart moves in straight line.

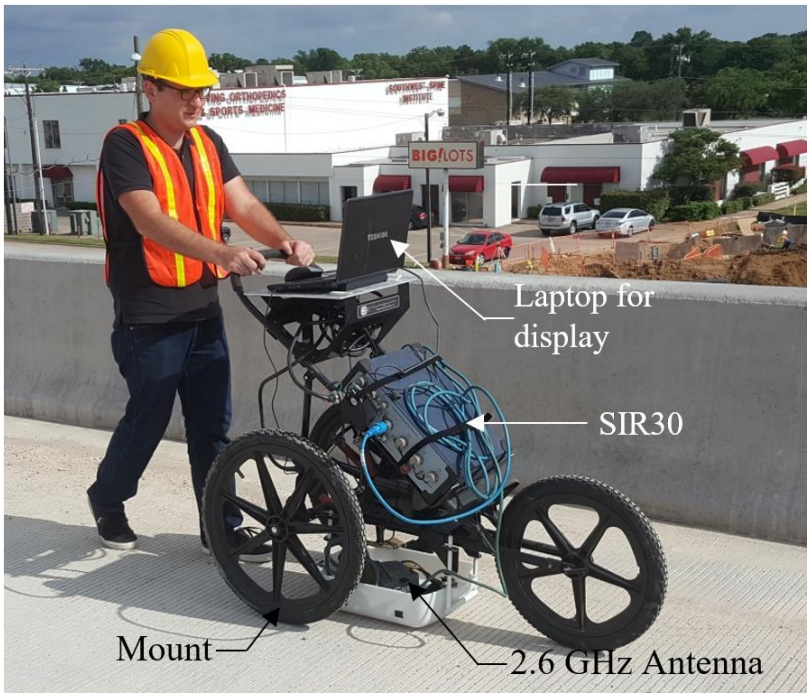

Figure 4-1 Tri-wheel Cart with Ground Coupled Antenna

The GPR setting for all four bridges is tabulated in Table 4-1. The GPR was set to collect data in distance mode with a survey wheel used for measurement. The survey wheel was calibrated so that distance measured should be equal to length driven or it will affect the calculation of dielectric constant with migration. The deck is scanned in the zig-zag pattern. For instance, scan #1 from start to end, scan #2 from end to start and so on as shown in Figure 4-2.

Table 4-1 GPR setting

scans/sec	scan/unit	units/mark	bits/sample
200	1	72	32

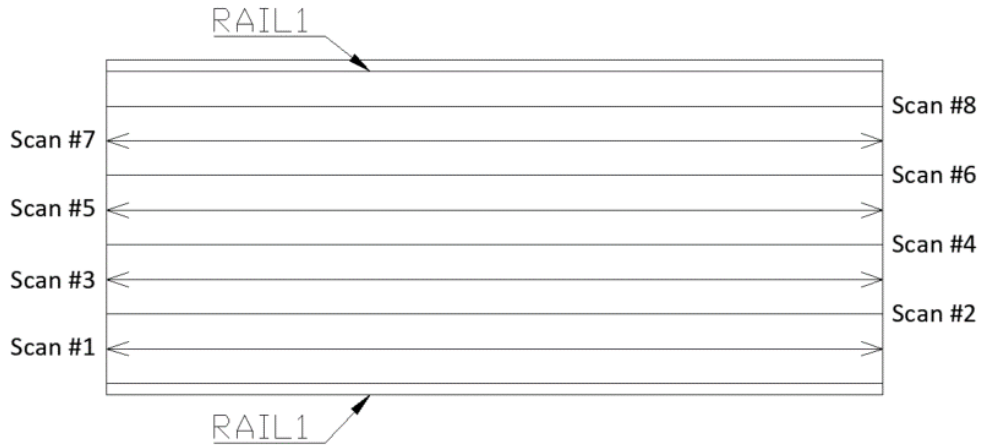

Figure 4-2 Typical Scanning Direction on Bridge Deck

After scanning, 1 to 3 individual rebars were located on deck and true depth or clear cover at this location were measured by drilling (Figure 4-3). This will be used later to calculate dielectric constant by ground truth method.

Figure 4-3 Drilling for true concrete cover

4.2 Post-Processing

GPR-SLICE (2018) software was used in post-processing the scan data. The steps include: 1) Importing data 2) Time zero correction; 3) Applying bandpass filter 4) Background removal filter; 5) Auto detection hyperbola, and 6) migration and ground truth method for determination of dielectric constant of concrete. The files from GPR is transferred into GPR-slice software to post process. Since the data is taken in the zig-zag pattern the alternate radargram is reversed and aligned to get all radargram in the same direction (Figure 4-4).

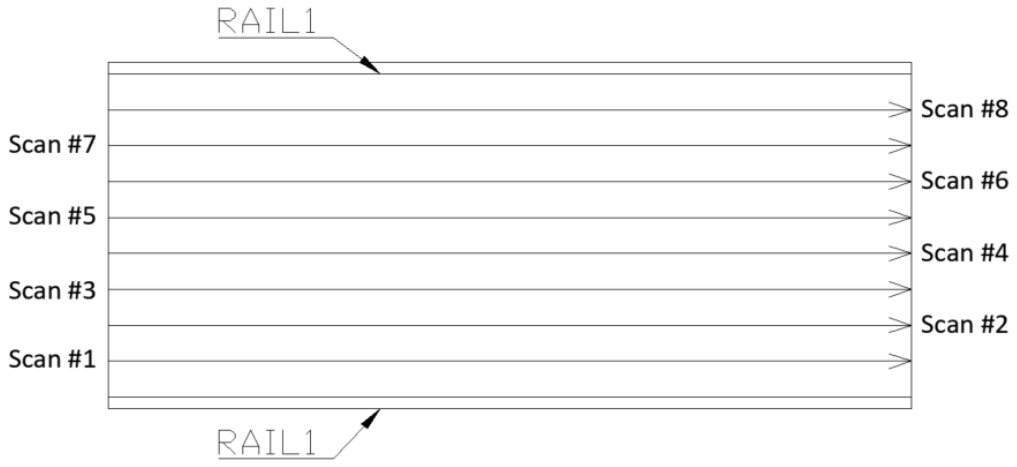

Figure 4-4 Aligning All Radargram In Same Direction

Time-zero correction refer to identification of true concrete surface which is first positive peak in radargram. This is set as a start line for TWTTs measurement. Figure 4-5 shows the B-scan on left and corresponding A-scan to the right. The first positive peak is marked with the black line which is starting axis for the measurement of TWTTs. The clear cover of rebar is equivalent to distance between two positive peaks in A-scan.

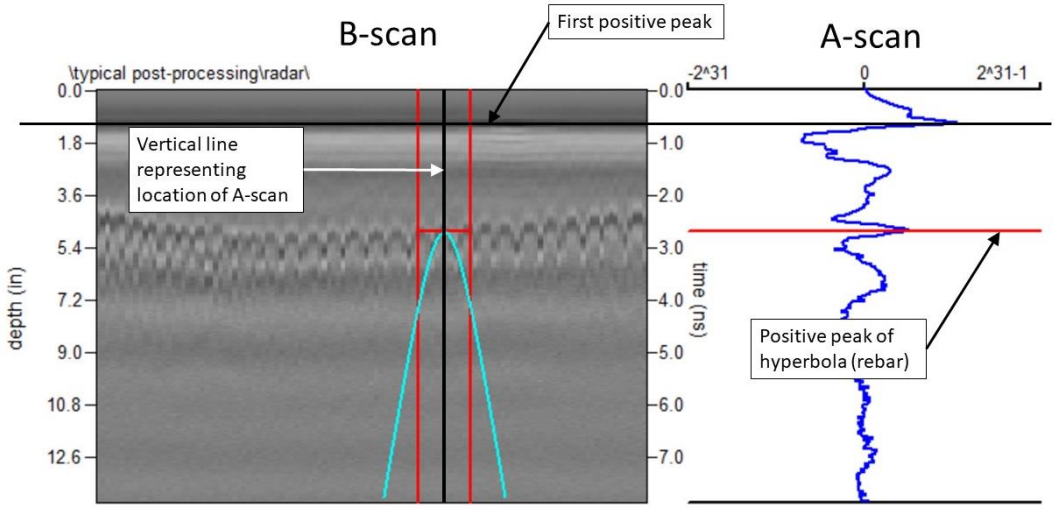

Figure 4-5 Measurement of Rebar Depth

For a particular radargram, there are 1 to 2 rebars or hyperbolas per foot which equal 150 to 480 hyperbolas per radargram dependent on the spacing of rebar and length of the bridge. For this auto-detection module of GPR-slice is used. The radargrams are filtered by the bandpass filter and background removal which aid in accurate detection. Even with the filters applied detection cannot be perfected (Figure 4-6). The peaks which are off are deleted and manually adjusted. This process is time-consuming so peaks between two linearly varying points are neglected. The information stored in '.dat' file is extracted for next step.

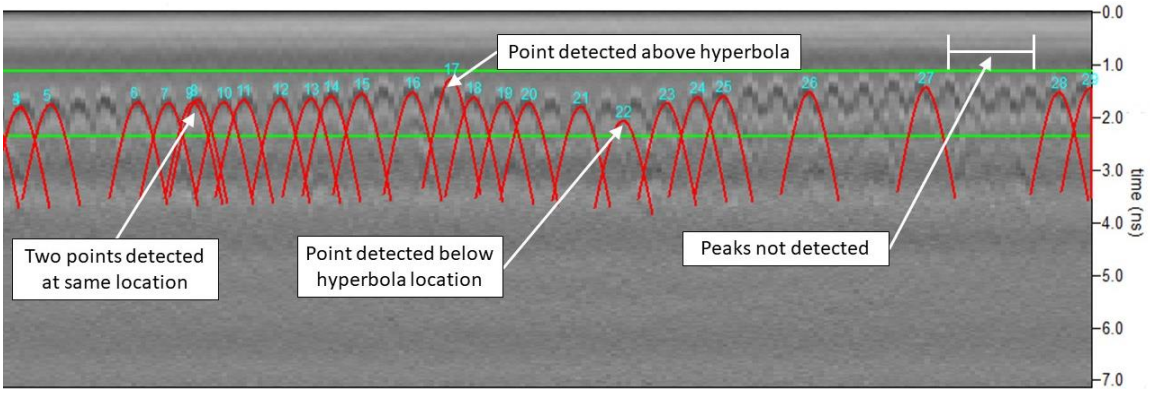

Figure 4-6 Auto-detection of Hyperbola

There was an error in the length of radargram of new SH183 over loop 12 eastbound, old SH183 over loop 12 east and westbound. Actual length scanned was not equal to radargram. The correction was done by locating the start and end of the bridge in radargram and scaling distance between them to match the actual scan (bridge) length. The absence of bottom rebar and presence of strong reflection due to the metallic expansion joint at the surface indicated start and end points. Figure 4-7 shows the line separating the approach slab there is no presence of second layer of rebar before this line and Figure 4-8 shows the end of the bridge with strong reflection by metal at the expansion joint.

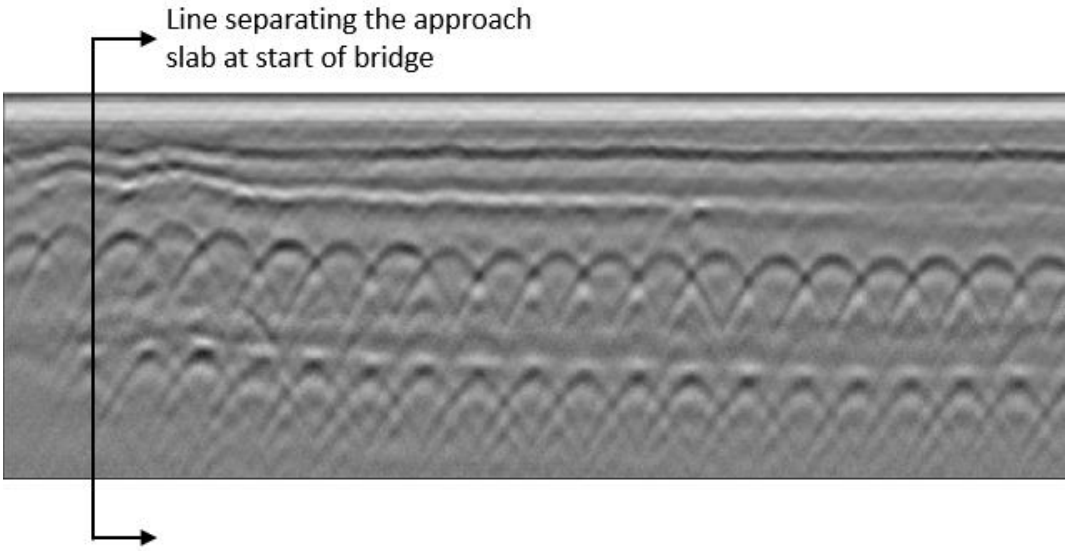

Figure 4-7 Line Separating the Approach Slab at Start of Bridge

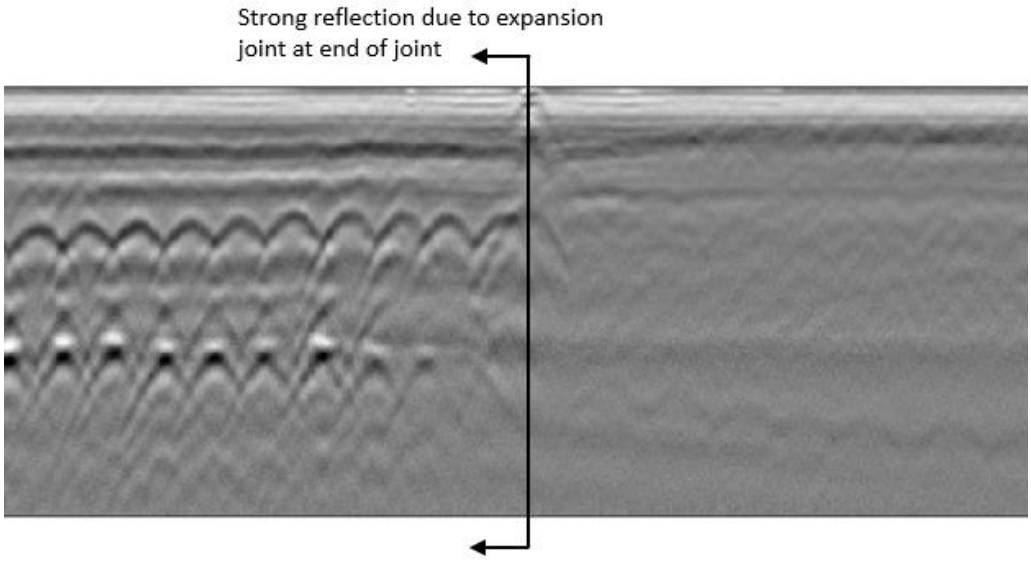

Figure 4-8 Strong Refection Denotes the Expansion Joint

There were no reflections of expansion joint in some radargram such radargram whole length were scaled and was not included in estimated of dielectric constant.

4.3 Determination of Dielectric Constant and Rebar Cover

Migration

As we know the GPR radiates radar waves in a wide cone. For a rebar at the middle of the cone (just beneath the antenna), the travel time of the wave (or distance) from the transmitter to the receiver will be less as compared to rebar situated at the end. While antenna is dragged, reflected pulses reach at the different interval by combining this hyperbolic pattern is formed. The velocity of the medium will determine the shape of the hyperbola. The medium with the slower velocities or high dielectric constant will produce narrow hyperbola and faster velocities or lower dielectric constant will produce broader hyperbola.

Migration is geophysical signal processing filter which collapses the hyperbola to a dot. To successfully achieve a dot the hyperbola in filter menu is matched with the hyperbola in radargram. The migrator width is set which refer to limit of migration filter length represented by two vertical lines. The TxxR which is distance between transmitter and receiver is input in column and is equal to (0.04m) for 2.6 GHz antenna. After applying this filter if hyperbola collapses to a dot the dielectric constant displayed in the column is selected, if not the hyperbola is slightly adjusted till bright dot is achieved. The depth is then calculated using with obtained dielectric constant and TWTTs of rebars with Equation 4-1.

$$d = \frac{c.t}{2\sqrt{\varepsilon}}$$

Equation 4-1 (Geophysical Archaeometry Laboratory Inc., 2018)

Where, d is clear cover of rebar.

Migration was applied to all four bridges and dielectric constant obtained is tabulated in Table 4-2.

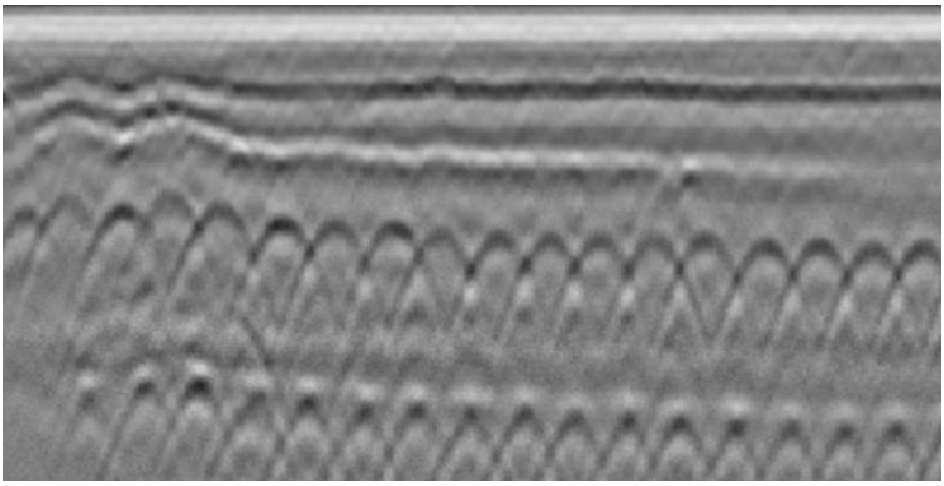

Figure 4-9 Before Migration

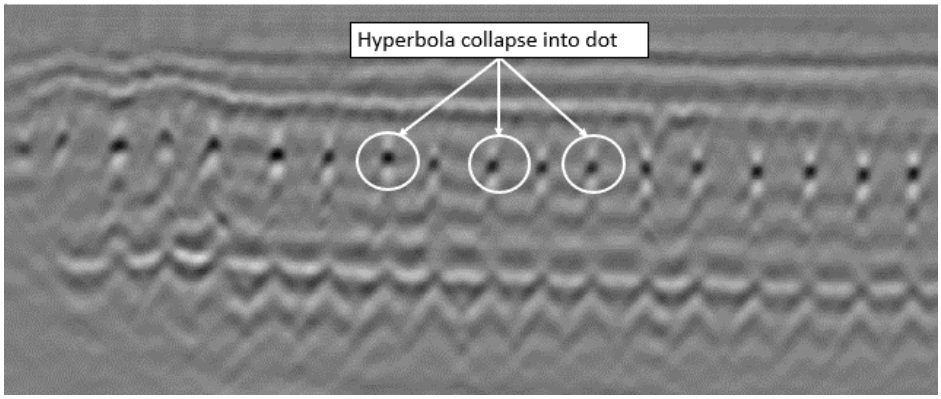

Figure 4-10 After migration

Table 4-2 Dielectric Constant from Migration

Bridge			Dielectric constant
SH 183 over Loop 12	Old	Eastbound	6.25
		Westbound	7.01
	New	Eastbound	8.27
		Westbound	8.38
SH 183 over MacArthur	Old	Eastbound	5.78
		Westbound	5.44
	New	Eastbound	10.46
		Westbound	9.37

Ground Truth

In ground truth method, a hyperbolic reflection of the drilled holes taken is located in radargram. From this TWTT is found out. With the actual cover of this rebar and TWTT known dielectric constant can be found by Equation 4-1. Since exactly locating this reflection is not possible considering a slight error in length. To overcome the rebars within ±1 feet (30.48 cm) are select and average TWTTs are taken into consideration. The dielectric constant calculated form truth depth is tabulated in Table 4-3.

Table 4-3 Dielectric constant by ground truth method

Bridge			**#Drills**	**Depth of rebar (in.)**	**TWTT (X10^{-9} second)**	**Dielectric constant**
SH 183 over Loop	Old	Eastbound	1	8.5 (216mm)	5.46	5.456
	New	Eastbound	1	4 (102mm)	7.44	7.441
			2	4.25 (108mm)	5.69	5.688
	New	Westbound	1	3.75 (95mm)	7.48	7.479
			2	3 (76mm)	7.52	7.523
SH 183 over MacArthur	Old	Eastbound	1	2.5 (64mm)	5.13	5.134
			2	2.4 (61mm)	6.68	6.676
	Old	Westbound	1	2.6 (66mm)	7.45	7.447
	New	Eastbound	1	3 (76mm)	13.37	13.374
			2	2.75 (70mm)	12.64	12.644
			3	2.4 (61mm)	12.62	12.621
	New	Westbound	1	2.5 (64mm)	11.31	11.309
			2	2.25 (57mm)	11.15	11.150

4.4 Gridding and Plotting Contours

After determining the rebar cover, the data is converted into a grid. Since the scans are taken 3 feet (91mm) apart in a transverse direction the rebar location between two scan lines are linearly interpolated. Triangulation with linear interpolation method in Surfer software v15 (Golden software) is used for interpolation. This method does not

extrapolate beyond limits and is best suited to interpolate rebar cover data. This grid data is then plotted in form of contours discuss in results.

Chapter 5

Deck Design moments

5.1 Total Factored Designed Negative Moment

For calculation of total factored negative bending moments, the AASTHO appendix A4-1 (AASHTO, 2017) deck design table. The moments are calculated using the equivalent strip method as applied to concrete slabs supported on parallel girders. The girder all brides are parallel and can be assumed parallel for new SH183 over MacArthur. Multiple presence factors and dynamic load allowance are included in the tabulated values.

The method requires:

- Deck supported on more than three girders and having a width of not less than 14 ft between the centerlines of the exterior girder.
- For overhang, minimum total overhang width of 21 in. (0.53m) is measured from center of the exterior girder and maximum equal to or smaller of 0.625 times the girder spacing or 6 ft.

All the requirements are satisfied for all bridges. Since, there is variation in girder spacing for different spans maximum spacing between girders in a span was considered for design moment calculation and is tabulated in Table 5-1.

Table 5-1 Maximum Girder Spacing

Bridge			Span number	Girder Spacing(ft.)
SH 183 over Loop	Old	Eastbound	Span 1	5.5 (1.68m)
		Westbound	Span 1	5.917 (1.8m)
	New	Eastbound	Span 1	6.789 (2.07m)
			Span 2	10.448 (3.18m)
		Westbound	Span 1	7 (2.13m)
			Span 2	8.85 (2.7m)
SH 183 over MacArthur	Old	Eastbound	Span 1	8 (2.44m)
		Westbound	Span 1	8 (2.44m)
	New	Eastbound	Span 1	11.422 (3.48m)
			Span 2	6.6 (2.01m)
			Span 3	11.664 (3.56m)

The concrete of compressive strength f'_c = 4 ksi (27.57 N/mm^2) and steel fy = 60ksi (0.413 kN/m^2)was used in all bridges. The unit weight of concrete 0.145 kcf (22.77 kN/mm^3) was obtained from AASTHO Table 3.5.1-1 for $f'_c \leq 5$ ksi (34.47 N/mm^2). Being conservative future wearing surface load were assumed 0.025 k/ft (0.036 kN/m). The deck thickness and dead load tabulated in Table 5-2.

Table 5-2 Dead Load of Slab and Wearing Surface

Bridge			Thickness of deck (in.)	Dead load (k/ft)
SH 183 over Loop	Old	Eastbound	6 (152mm)	0.073 (1.07kN/m)
		Westbound	6 (152mm)	0.073 (1.07kN/m)
	New	Eastbound	8.5 (216mm)	0.103 (1.5kN/m)
		Westbound	8.5 (216mm)	0.103 (1.5kN/m)
SH 183 over MacArthur	Old	Eastbound	6.5 (165mm)	0.079 (1.15kN/m)
		Westbound	6.5 (165mm)	0.079 (1.15kN/m)
	New	Eastbound	8.5 (216mm)	0.103 (1.5kN/m)
		Westbound	8.5 (216mm)	0.103 (1.5kN/m)

Table 5-3 Negative Bending due to Dead Load and Future Wearing Surface

Bridge			Span number	Girder Spacing(ft.)	Negative bending moment (k-ft)	
					Dead load	Future wearing surface
SH 183 over Loop	Old	Eastbound	Span 1	5.5 (1.68m)	0.186 (0.25kNm)	0.064 (0.09kNm)
		Westbound	Span 1	5.917 (1.8m)	0.216 (0.29kNm)	0.074 (0.1kNm)
	New	Eastbound	Span 1	6.789 (2.07m)	0.402 (0.55kNm)	0.098 (0.13kNm)
			Span 2	10.448 (3.18m)	0.953 (1.29kNm)	0.232 (0.31kNm)
		Westbound	Span 1	7 (2.13m)	0.505 (0.68kNm)	0.81 (1.1kNm)
			Span 2	8.85 (2.7m)	0.104 (0.14kNm)	0.166 (0.23kNm)
SH 183 over MacArthur	Old	Eastbound	Span 1	8 (2.44m)	0.817 (1.11kNm)	0.275 (0.37kNm)
		Westbound	Span 1	8 (2.44m)	0.817 (1.11kNm)	0.275 (0.37kNm)
	New	Eastbound and Westbound	Span 1	11.422 (3.48m)	1.139 (1.54kNm)	0.277 (0.38kNm)
			Span 2	6.6 (2.01m)	0.38 (0.52kNm)	0.093 (0.13kNm)
			Span 3	11.664 (3.56m)	1.188 (1.61kNm)	0.289 (0.39kNm)

The distance between the center of the girder to the location of design sections for negative moments in the deck is given in article 4.6.2.1.6. It is one-third the flange width, but not exceeding 15 ft. (case k) for precast I-shaped concrete beams applicable to new MacArthur, both old and new loop 12 bridges. Old MacArthur had monolithic construction design section is at the face of support (case e). In Table 5-4 below, type of girders and design sections is tabulated.

Table 5-4 Design Sections for Live Load Calculation

Bridge			Span number	Supporting component/ type of deck	Flange width/ beam width (in)	Design section (in)
SH 183 over Loop	Old	Eastbound	Span 1	Precast bulb tee/Cast-in-place	12 (304.8mm)	4 (101.6mm)
		Westbound	Span 1		12 (304.8mm)	4 (101.6mm)
	New	Eastbound	Span 1		36 (914.4mm)	12 (304.8mm)
			Span 2		36 (914.4mm)	12 (304.8mm)
		Westbound	Span 1		36 (914.4mm)	12 (304.8mm)
			Span 2		36 (914.4mm)	12 (304.8mm)
SH 183 over MacArthur	Old	Eastbound	Span 1	Cast-in-place concrete Tee beam/monolithic	11 (279.4mm)	11 (279.4mm)
		Westbound	Span 1		11 (279.4mm)	11 (279.4mm)
	New	Eastbound and Westbound	Span 1	Precast bulb tee/Cast-in-place	36 (914.4mm)	12 (304.8mm)
			Span 2		36 (914.4mm)	12 (304.8mm)
			Span 3		36 (914.4mm)	12 (304.8mm)

The live load moments are calculated from AASTHO Table 4-1 from interpolation and is tabulated in Table 5-5.

Table 5-5 Negative Live Load Moment

Bridge			Span number	Negative live load moment (k-ft)
SH 183 over Loop	Old	Eastbound	Span 1	3.52 (4.77kNm)
		Westbound	Span 1	3.89 (5.27kNm)
	New	Eastbound	Span 1	2.67 (3.62kNm)
			Span 2	4.96 (6.72kNm)
		Westbound	Span 1	2.84 (3.85kNm)
			Span 2	3.69 (5kNm)
SH 183 over MacArthur	Old	Eastbound	Span 1	3.62 (4.91kNm)
		Westbound	Span 1	3.62 (4.91kNm)
	New	Eastbound and Westbound	Span 1	6.1 (8.27kNm)
			Span 2	2.57 (3.48kNm)
			Span 3	6.37 (8.64kNm)

5.2 Total Factored Negative Bending Moment

The factor of 1.25, 1.5 and 1.75 is applied to dead, future wearing surface and live load bending moment Table 5-6.

Table 5-6 Total Negative Factored Bending Moments

Bridge			Span number	Total factored bending moment, Strength I (k-ft)
SH 183 over Loop	Old	Eastbound	Span 1	6.489 (8.8kNm)
		Westbound	Span 1	7.189 (9.75kNm)
	New	Eastbound	Span 1	5.324 (7.22kNm)
			Span 2	10.223 (13.86kNm)
		Westbound	Span 1	5.46 (7.4kNm)
			Span 2	9.94 (13.48kNm)
SH 183 over MacArthur	Old	Eastbound	Span 1	7.757 (10.52kNm)
		Westbound	Span 1	7.757 (10.52kNm)
	New	Eastbound and Westbound	Span 1	12.52 (16.97kNm)
			Span 2	5.112 (6.93kNm)
			Span 3	13.069 (17.72kNm)

5.3 Capacity of Deck

In this section deck factored flexural resistance (capacity) was calculated for proposed bridge deck and capacity for variable cover is discussed later. The capacity and depth of equivalent stress block is given by Equation 5-1 and Equation 5-2, respectively. The width of design section b= 12 in (305mm) and resistance factor for tensioned-controlled section 0.9 (AASTHO 5.5.4.2) was considered in calculation. Bridge specific parameters rebar size, spacing, deck thickness and top cover is listed in Table 5-7 and capacity is tabulated in Table 5-8.

$$\Phi \mathrm{M}_n = \Phi A_s f_y (\mathrm{d} - {}^{a}/_{2}) \qquad \text{Equation 5-1(Design of Highway Bridges, 2013)}$$

And

$$a = \frac{A_s f_y}{0.85 f'_c b} \qquad \text{Equation 5-2(Design of Highway Bridges, 2013)}$$

Table 5-7 Summary of top transverse spacing and cover

Bridge			Span number	Rebar size	Spacing of top rebar (in)	Deck thickness, D (in)	Top clear cover (in)
SH 183 over Loop	Old	Eastbound	Span 1	5	13 (330mm)	6 (152mm)	2 (51mm)
		Westbound	Span 1	5	13 (330mm)	6 (152mm)	2 (51mm)
	New	Eastbound	Span 1	5	6 (152mm)	8.5 (216mm)	2.5 (64mm)
			Span 2	5	6 (152mm)	8.5 (216mm)	2.5 (64mm)
		Westbound	Span 1	5	6 (152mm)	8.5 (216mm)	2.5 (64mm)

			Span 2	5	6 (152mm)	8.5 (216mm)	2.5 (64mm)
SH 183 over MacArthur	Old	Eastbound	Span 1	5	13 (330mm)	6.5 (165mm)	2 (51mm)
		Westbound	Span 1	5	13 (330mm)	6.5 (165mm)	2 (51mm)
	New	Eastbound and Westbound	Span 1	5	5.25 (133mm)	8.5 (216mm)	2.5 (64mm)
			Span 2	5	6 (152mm)	8.5 (216mm)	2.5 (64mm)
			Span 3	5	5.25 (133mm)	8.5 (216mm)	2.5 (64mm)

Table 5-8: Proposed deck capacity

Bridge			**ΦM_n (k-ft)**
SH 183 over Loop	Old	Eastbound	4.748 (6.44kNm)
		Westbound	4.748 (6.44kNm)
	New	Eastbound	15.868 (21.51kNm)
			15.868 (21.51kNm)
		Westbound	15.868 (21.51kNm)
			15.868 (21.51kNm)
SH 183 over MacArthur	Old	Eastbound	5.392 (7.31kNm)
		Westbound	5.392 (7.31kNm)
	New	Eastbound and Westbound	18.135 (24.59kNm)
			15.868 (21.51kNm)
			18.135 (24.59kNm)

The proposed deck negative moment capacity and total factored bending moment due to strength I is summarized in the Table 5-9. Old bridges negative moment capacity was found out to be less than total factored design moment because the old bridges was designed for light weight HS-20 as compared to heavy weight HL-93. As the

strip is considered 1 feet (305mm) within this two-rebar lying in it can be at different cover depth. This variation was not considered in calculation.

Table 5-9: Total Factored Design and Negative Moment Capacity

Bridge			Span number	Total factored design moment, Strength I (k-ft)	Negative moment capacity (k-ft)	Difference (k-ft)
SH 183 over Loop	Old	Eastbound	Span 1	6.489 (8.8kNm)	4.748 (6.44kNm)	1.741 (2.36kNm)
		Westbound	Span 1	7.189 (9.75kNm)	4.748 (6.44kNm)	2.441 (3.31kNm)
	New	Eastbound	Span 1	5.324 (7.22kNm)	15.868 (21.51kNm)	-10.544 (-14.3kNm)
			Span 2	10.223 (13.86kNm)	15.868 (21.51kNm)	-5.645 (-7.65kNm)
		Westbound	Span 1	5.46 (7.4kNm)	15.868 (21.51kNm)	-10.408 (-14.11kNm)
			Span 2	9.94 (13.48kNm)	15.868 (21.51kNm)	-5.928 (-8.04kNm)
SH 183 over MacArthur	Old	Eastbound	Span 1	7.757 (10.52kNm)	5.392 (7.31kNm)	2.365 (3.21kNm)
		Westbound	Span 1	7.757 (10.52kNm)	5.392 (7.31kNm)	2.365 (3.21kNm)
	New	Eastbound and Westbound	Span 1	12.52 (16.97kNm)	18.135 (24.59kNm)	-5.615 (-7.61kNm)
			Span 2	5.112 (6.93kNm)	15.868 (21.51kNm)	-10.756 (-14.58kNm)
			Span 3	13.069 (17.72kNm)	18.135 (24.59kNm)	-5.066 (-6.87kNm)

Chapter 6

Result and Discussion

The contours and rebar distribution of individual bridges are discussed in this section. The vertical and horizontal axis is the width and length in feet of the bridge, respectively. The contours are formed by joining equal cover interpolated points. The area with low and high covers are represented with cooler and hotter colors, respectively. All contours are aligned to north direction. The proposed clear cover during design phase of the bridges are tabulated in Table 6-1 and Table 6-2.

Table 6-1: Proposed clear cover for old bridges

Old Bridge	Asphalt overlay thickness (in.)	Proposed clear cover (in.)	Total cover (in.)
SH 183 over Loop	3	2	5
SH 183 over MacArthur	1.5	2	3.5

Table 6-2: Proposed clear cover for new bridges

New Bridge	Proposed clear cover (in.)
SH 183 over Loop	2.5
SH 183 over MacArthur	2.5

TxDOT Standard Specification 2014 states that the clear cover tolerance for the top mat reinforcement is +1/2 in. (13mm) and a minimum of 1 in. (25.4mm) is suggested. According to the American Concrete Institute Specification for Tolerances for Concrete Construction and Materials (ACI-117-10), the deck reinforcement cover is +1 in (25.4mm). No tolerance allowed in an upward direction.

The dielectric constant was calculated from migration. The Table 6-3 is the comparison of the dielectric constant from ground truth and migration. Neglecting the

values with the high dielectric constant value the deviation was less than 3.7. Due to uncertainty in locating exact drilled rebar dielectric constant from migration was adopted to calculated cover and corresponding contours.

Table 6-3: Comparison of dielectric constant form migration and ground truth

Bridge			Dielectric constant		Deviation
			Migration	Ground truth	
SH 183 over Loop	Old	Eastbound	6.25	5.46	0.80
		Westbound	7.01	6.2	0.81
	New	Eastbound	8.28	7.44	0.84
				5.69	2.59
		Westbound	8.38	4.83	3.55
				7.48	0.90
				7.52	0.86
SH 183 over MacArthur	Old	Eastbound	5.78	2.08	3.70
				5.13	0.65
				6.68	0.90
		Westbound	5.44	16.26	10.82
				7.45	2.01
				47.02	41.58
	New	Eastbound	10.46	13.37	2.91
				12.64	2.18
				12.62	2.16
		Westbound	9.37	6.69	2.68
				11.31	1.94
				11.15	1.78

6.1 New SH183 Over Loop 12 Eastbound

The Figure 6-1 is the contour of the bridge new SH183 over loop 12 eastbound. The rebar distribution is shown is Figure 6-2. Rebar cover was rounded off to nearest interval. The rebar varies from 1.5 to 4 inch (38 to 102mm) throughout the bridge. According to tolerance, the percent rebar distribution 29.03% lies within tolerance provided by TxDOT Standard Specification and 71.02% lies within the tolerance of +1 in. (25.4mm) provided by ACI-117-10.

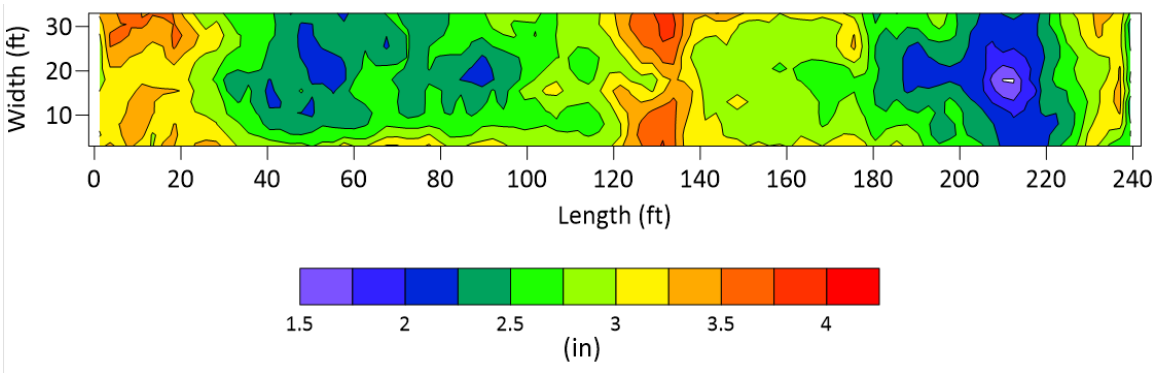

Figure 6-1 New SH183 over Loop 12 Eastbound

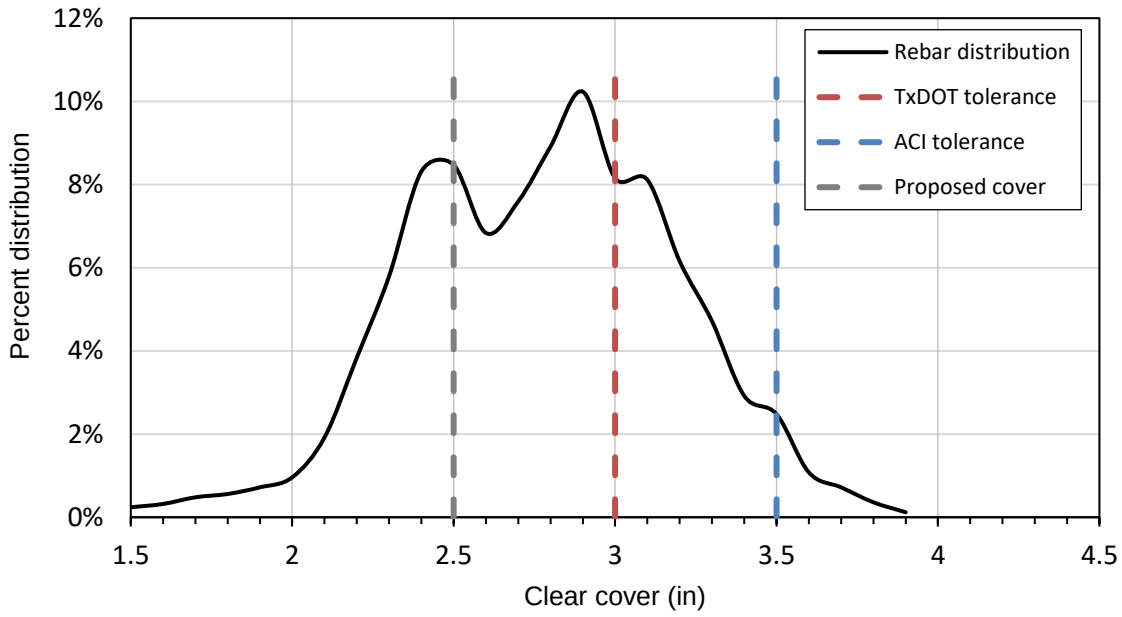

Figure 6-2: New SH183 over Loop 12 Eastbound Rebar Distribution

6.2 New SH183 Over Loop 12 Westbound

Figure 6-3 is the contour of SH183 over loop 12 .Figure 6-4 is the cover distribution ranging from 1.5 to 4.5-inch (38 to 114mm), with 43.59% and 73% lying ½ in. (13mm) and 1-inch (25.4mm) tolerance, respectively.

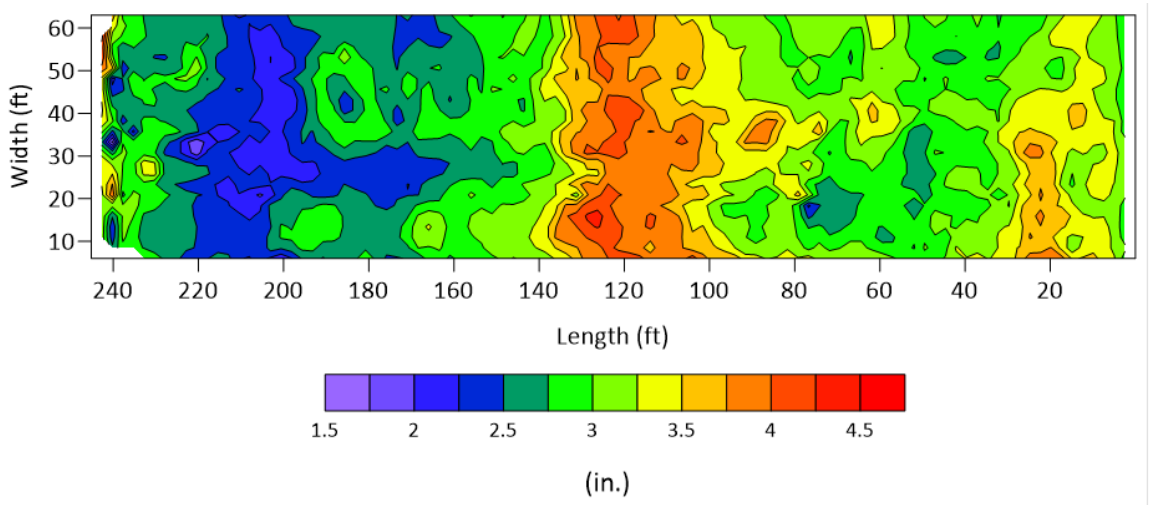

Figure 6-3 New SH183 Over Loop 12 Westbound

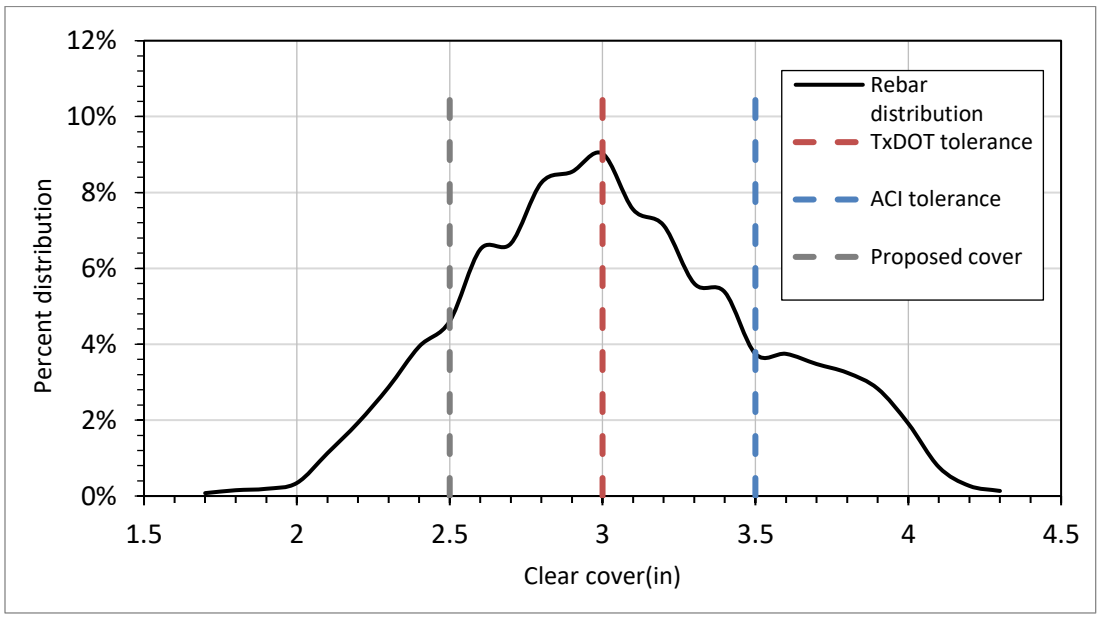

Figure 6-4 New SH183 Over Loop 12 Westbound Rebar Distribution

The Figure 6-5 is the comparison of design negative bending moment and the capacity of the deck. It can be observed that design negative moment is less than the reduced capacity due to variation. This suggest that the deck is safe even with the max cover range. This also implies that deck is over designed.

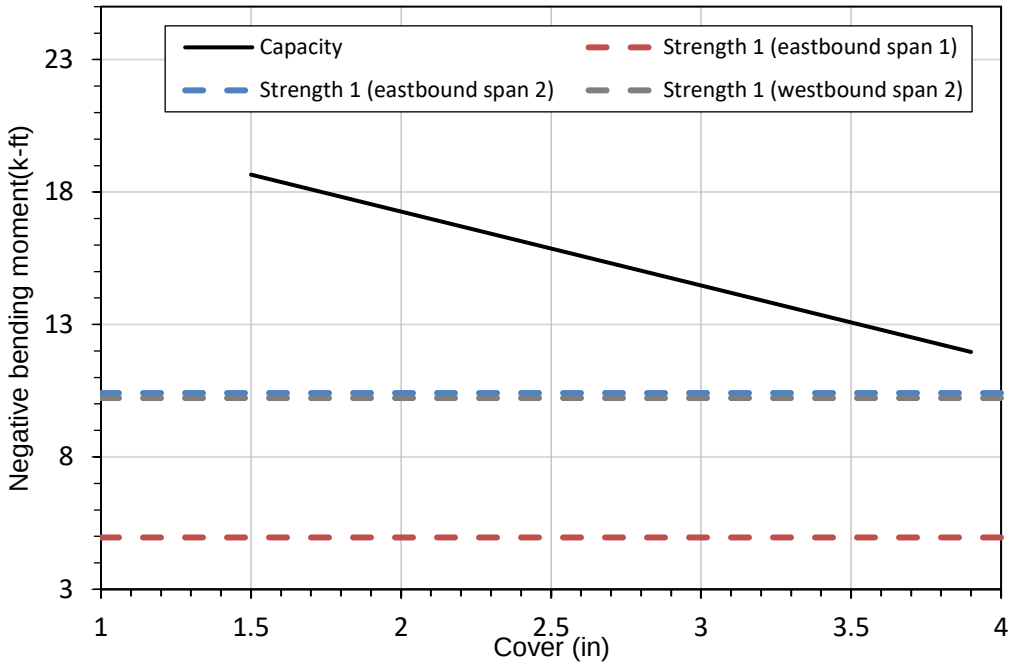

Figure 6-5 Negative bending moment vs clear cover

6.3 Old SH183 Over Loop 12 Eastbound

The old Loop 12 bridges had asphalt overlay on top. Figure 6-6 shows the variation of the interface between asphalt and concrete in old SH183 over Loop 12 bridges followed by the rebar hyperbolic reflection. The estimation of asphalt thickness was limited due to unclear (Figure 6-7) and not visible (Figure 6-8) interface in some location of radargram. This happens due to the interference of GPR waves with nearby radio waves emitted by mobile phones or TV antennas. Neglecting this area, the asphalt layer variation was found within 1.11 to 1.58 TWTTs which is equivalent to 3 to 4-in (76 to

102mm) thickness considering 5 as asphalt dielectric constant mention in GSSI RADAN 7 manual. This is approximate, for exact determination of the dielectric constant of asphalt actual thickness by drilling is needed which was not available in this case. The distribution without asphalt can be estimated by subtracting 3 to 4-in. (76-102mm) layer with combined depth.

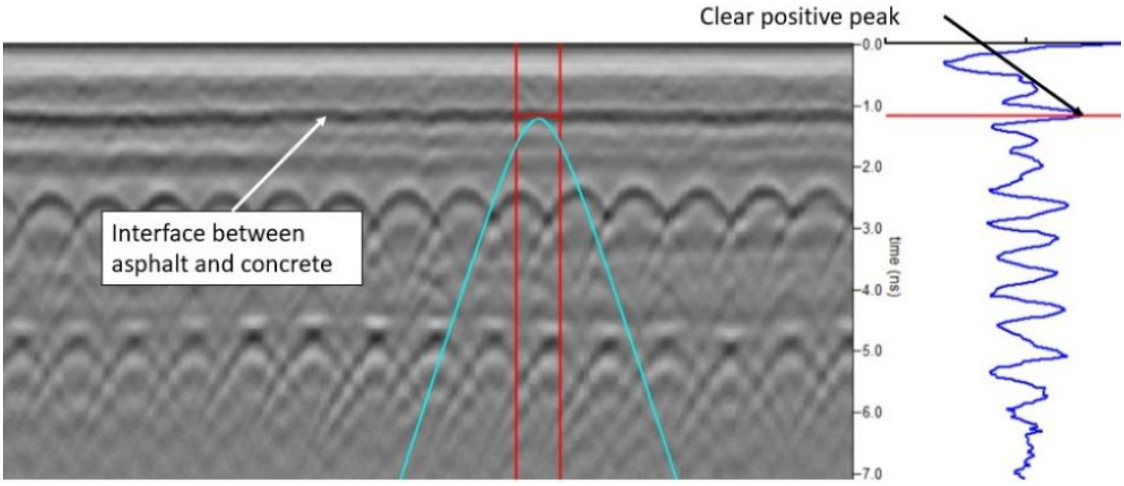

Figure 6-6 Interface Between Asphalt and Concrete

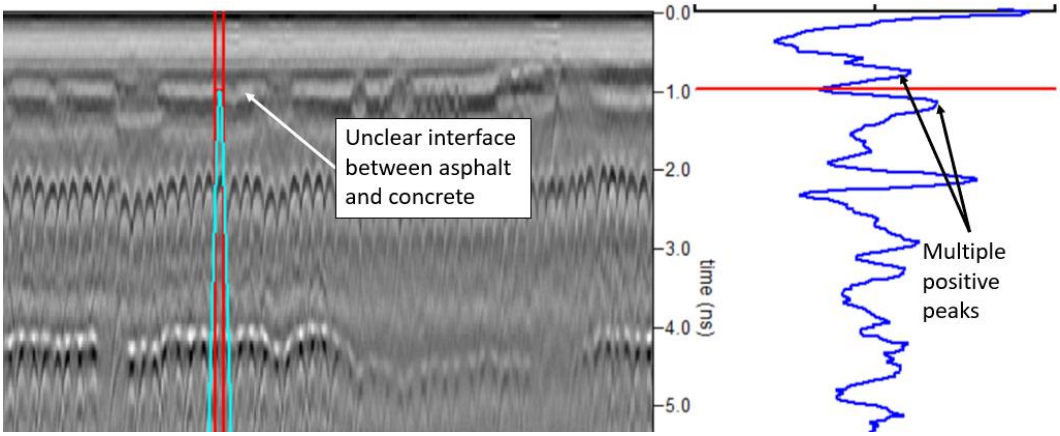

Figure 6-7 Unclear Interface Between Asphalt and Concrete

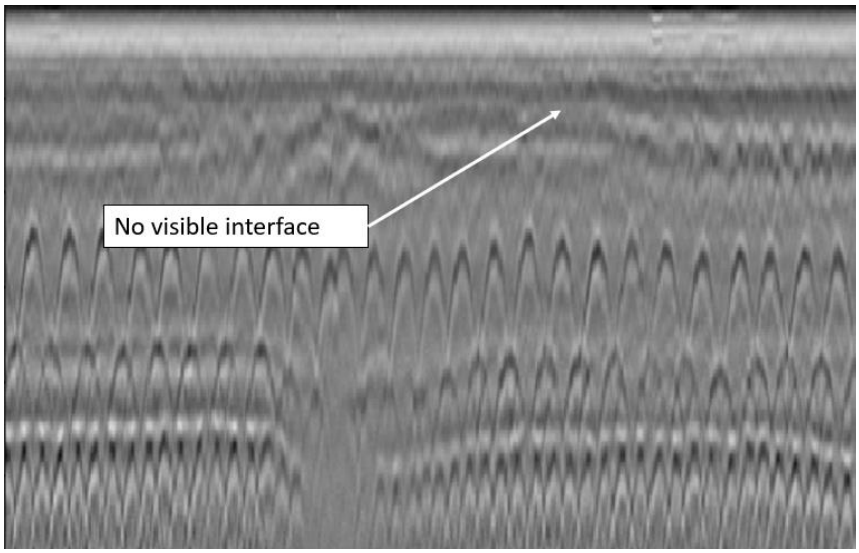

Figure 6-8 No Visible Interface

The contour (Figure 6-9) of old Loop 12 bridges is the sum of the asphalt layer and the concrete on top of rebar. It was observed that the rebar variation was within range 3.5 to 7-inch (89 to 178mm) (Figure 6-10). The part SH183 over Loop 12 was impact damaged was repaired in 2006. So, the concrete in that replaced part has different dielectric properties. This can be observed in the repaired area marked in Figure 6-11, where there is a sudden change in contour. The low cover was found mostly in repaired area. The distribution without asphalt was found within range 0.6 to 3 in. (15 to 76mm).

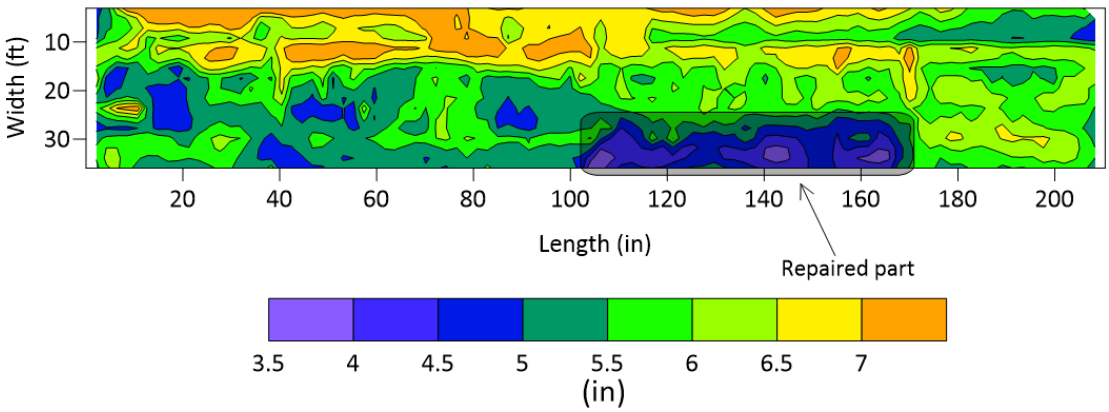

Figure 6-9 Old SH183 Over Loop 12 Eastbound

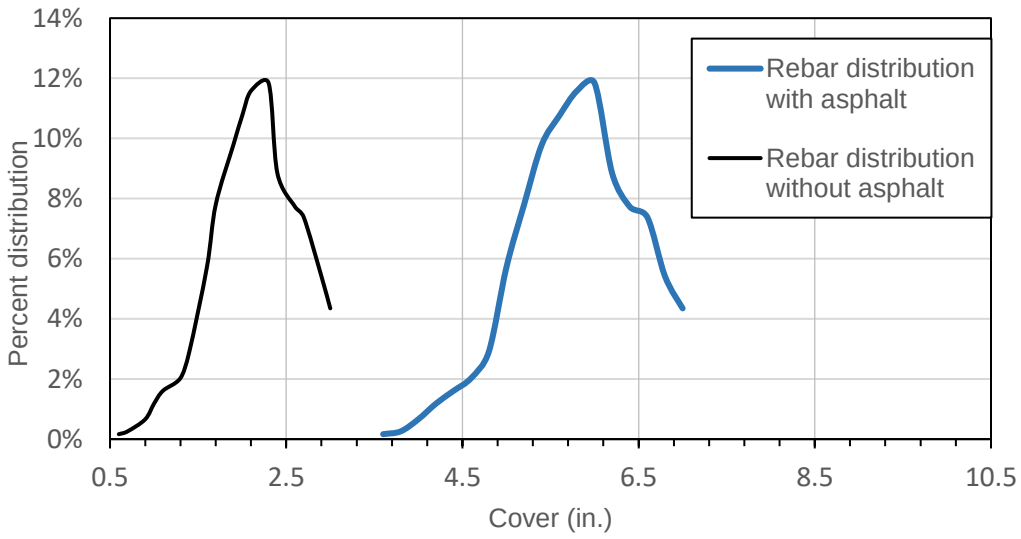

Figure 6-10 Old SH183 Over Loop 12 Eastbound Rebar Distribution

6.4 Old SH183 over loop 12 eastbound repaired part

Despite of the difference in concrete properties in repaired region the migration gave almost same dielectric constant of 6.28. Actual depth by drilling was suggested in this region to accurately determine depth of rebars in this region. The isolated contour

and the rebar distribution are shown in Figure 6-11 and Figure 6-12, respectively. It is observed the rebar variation is found with range 3-6-inch (76 to 152mm).

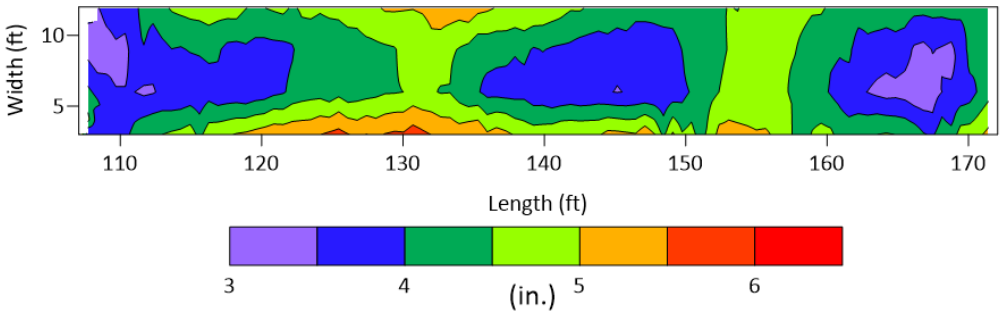

Figure 6-11 Repaired Part

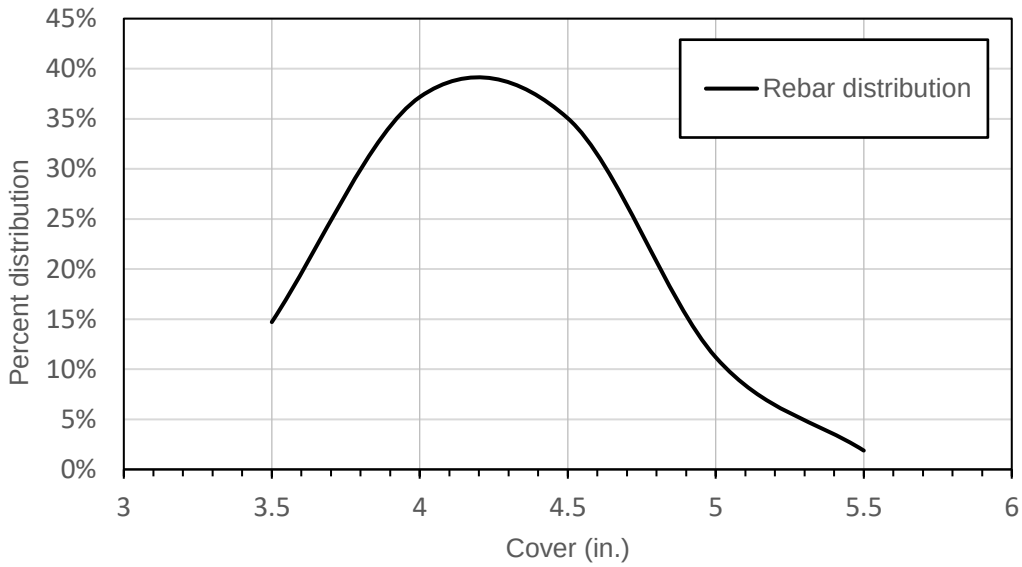

Figure 6-12 Repaired Part Rebar Distribution

6.5 Old SH183 over Loop 12 Westbound

Old SH183 over loop 12 westbound contours (Figure 6-13) showed the rebar variation within 4-7-in. (102 to 178mm) including the variation in asphalt layer(Figure

6-14). The distribution without asphalt layer was found within 1.3 to 3.3 inch (33 to 84mm). Figure 6-15 is the capacity vs design moment comparison.

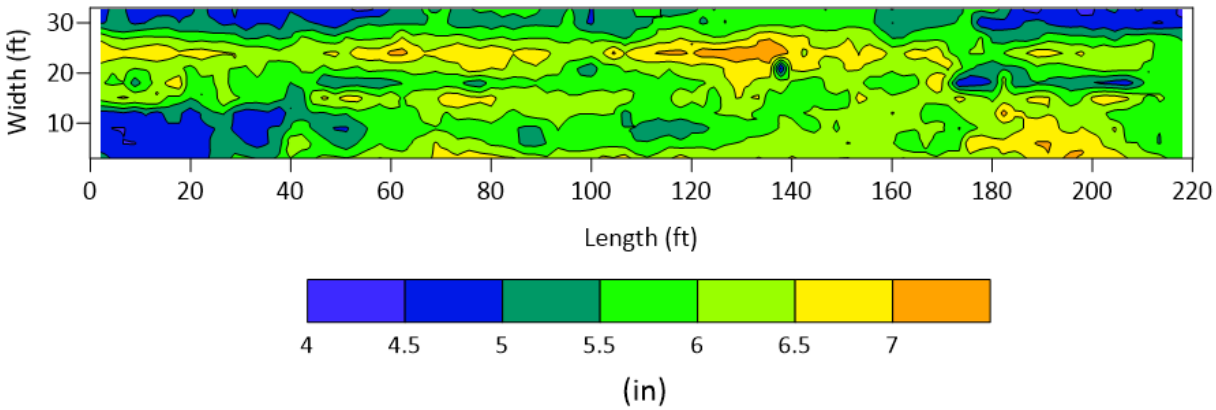

Figure 6-13 Old SH183 Over Loop 12 Westbound

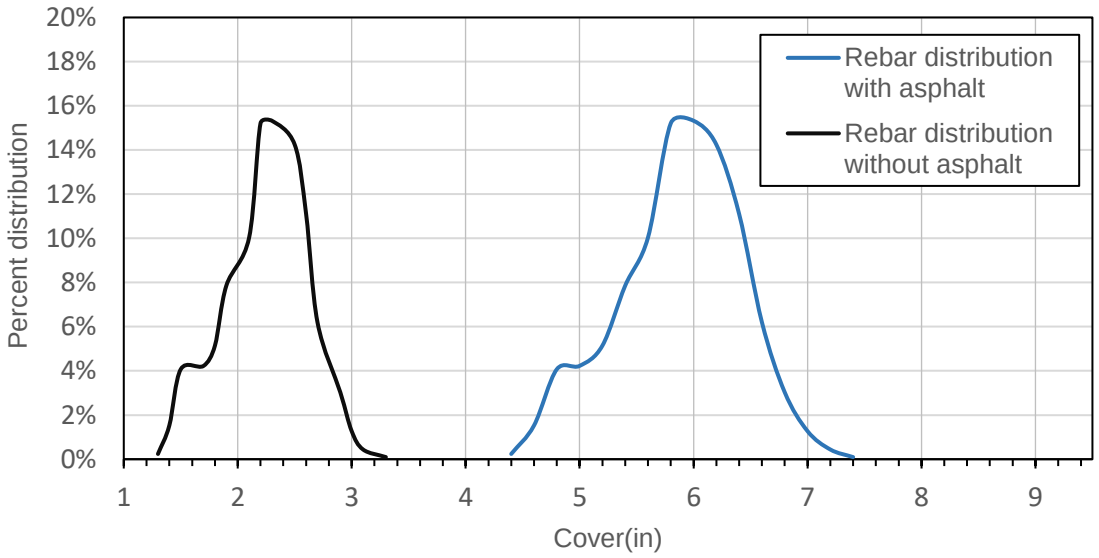

Figure 6-14 Old SH183 Over Loop 12 Westbound Rebar Distribution

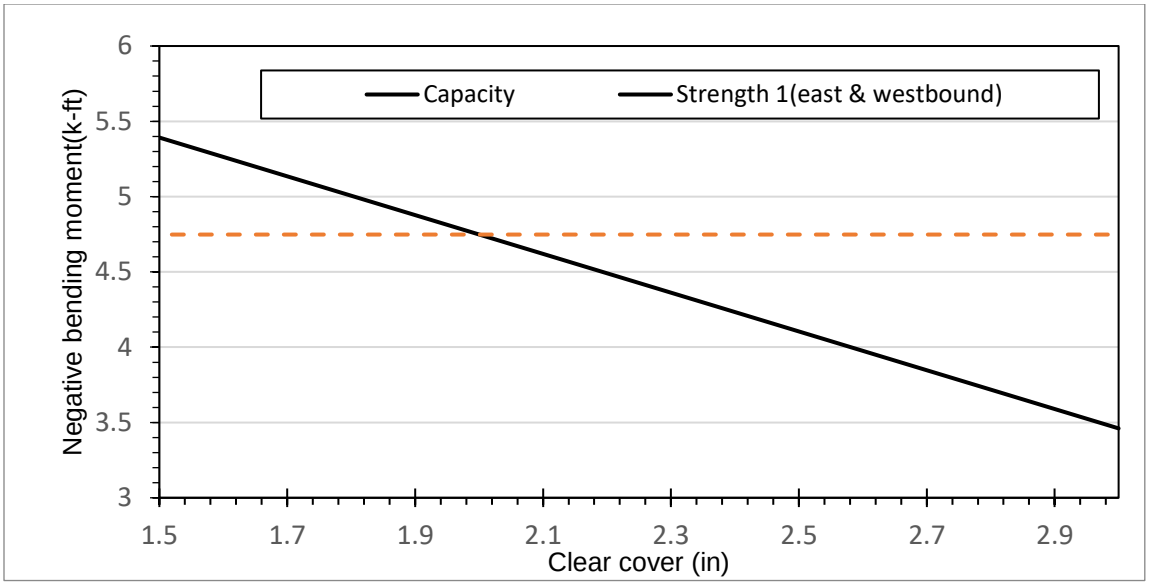

Figure 6-15 Old SH183 over Loop 12 Capacity vs Negative bending moment comparison

The Figure 6-16 is the contour of SH183 over MacArthur eastbound. The data before at start and after the end of the expansion joint was not included so the bridge contour appears skewed. The rebar variation ranged between 1.5 to 5 in. (38 to 127mm) with 38.04% and 75.97% within TxDOT and ACI tolerances (Figure 6-17) was observed.

6.6 New SH183 over MacArthur Eastbound

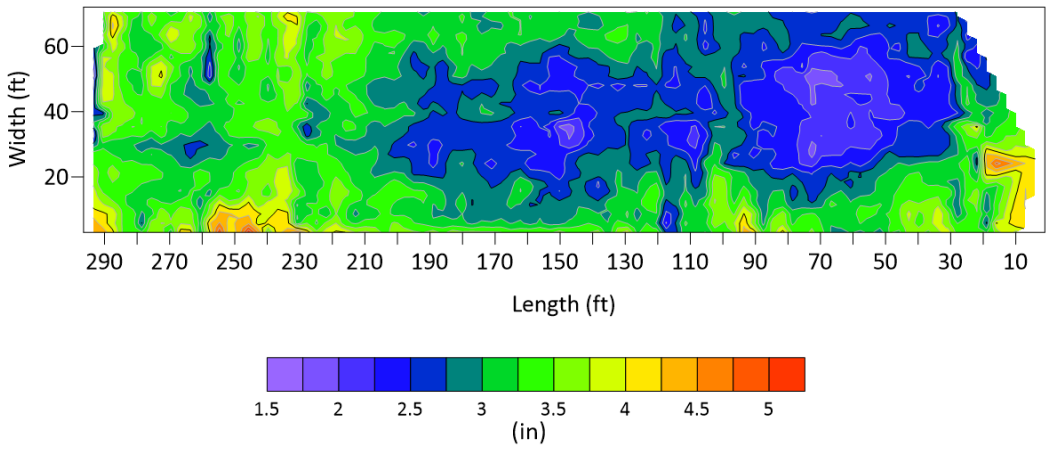

Figure 6-16 New SH183 over MacArthur Eastbound

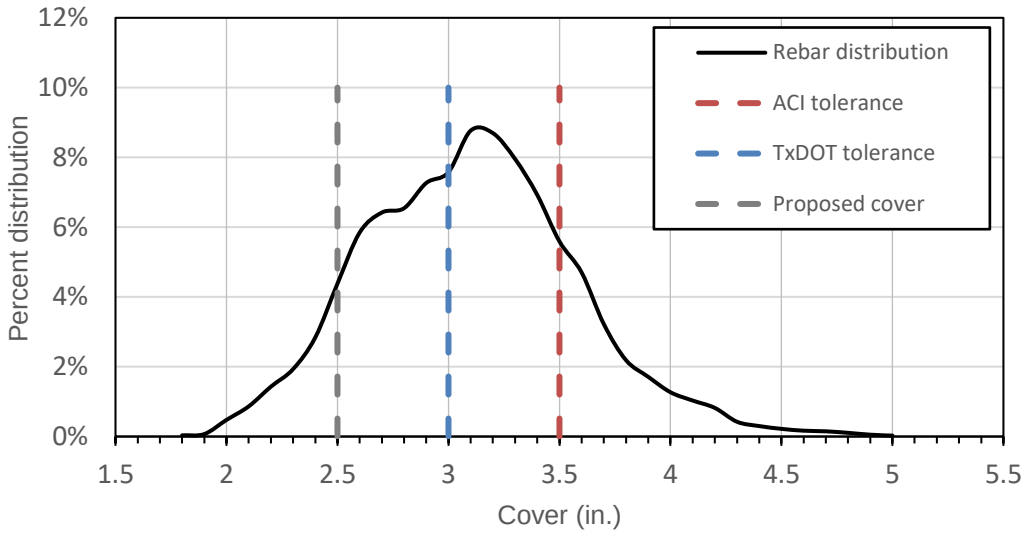

Figure 6-17 New SH183 over MacArthur Eastbound Rebar Distribution

6.7 New SH183 over MacArthur Westbound

Figure 6-18 is the contour of new SH183 over MacArthur westbound. The rebar variation was found within limits 2 to 4 in. (51 to 102mm) and the percent distribution (Figure 6-19) was found 50.65% and 86.70% within TxDOT and ACI-117 specifications, respectively. It can be observed from Figure 6-20 that the cover beyond 4 in (102mm). reduce capacity beyond design moment which is failure of bridge in strength.

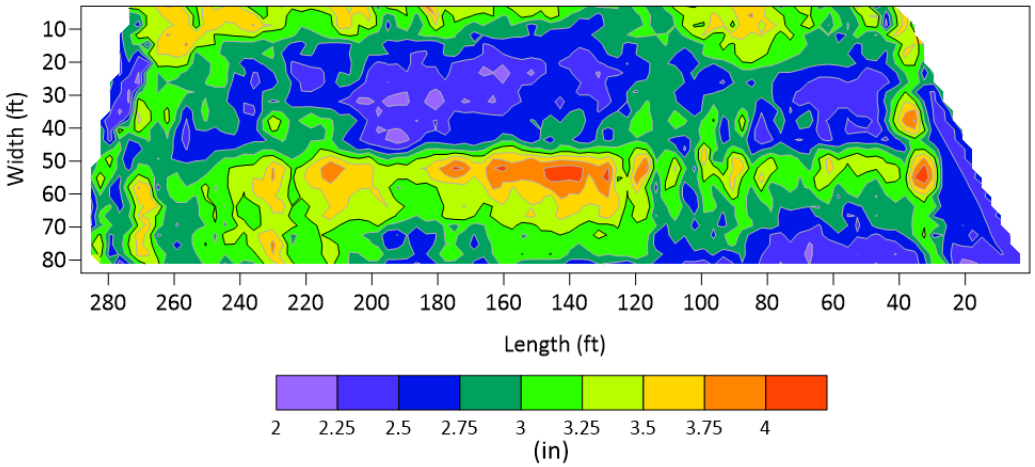

Figure 6-18 New SH183 over MacArthur Westbound

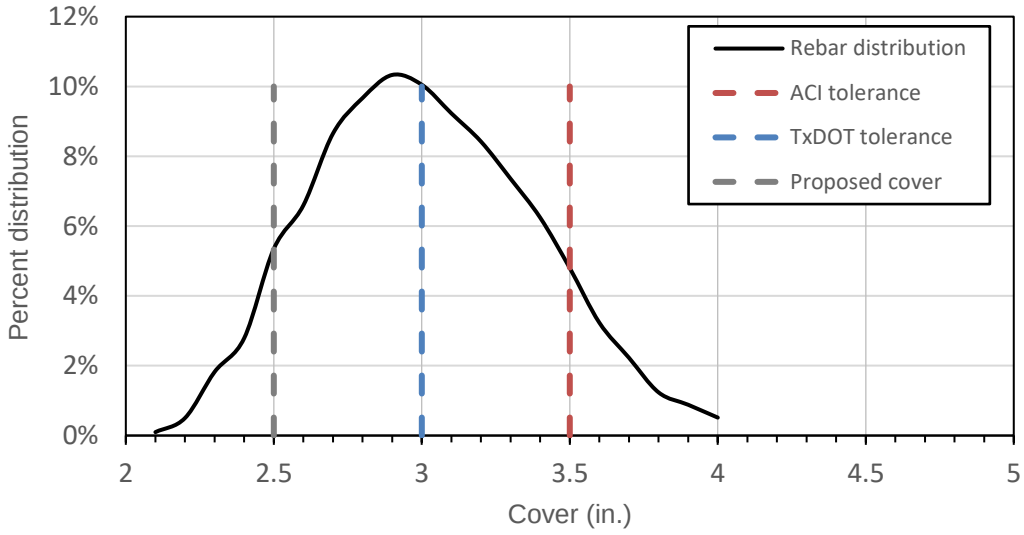

Figure 6-19 New SH183 over MacArthur Westbound Rebar Distribution

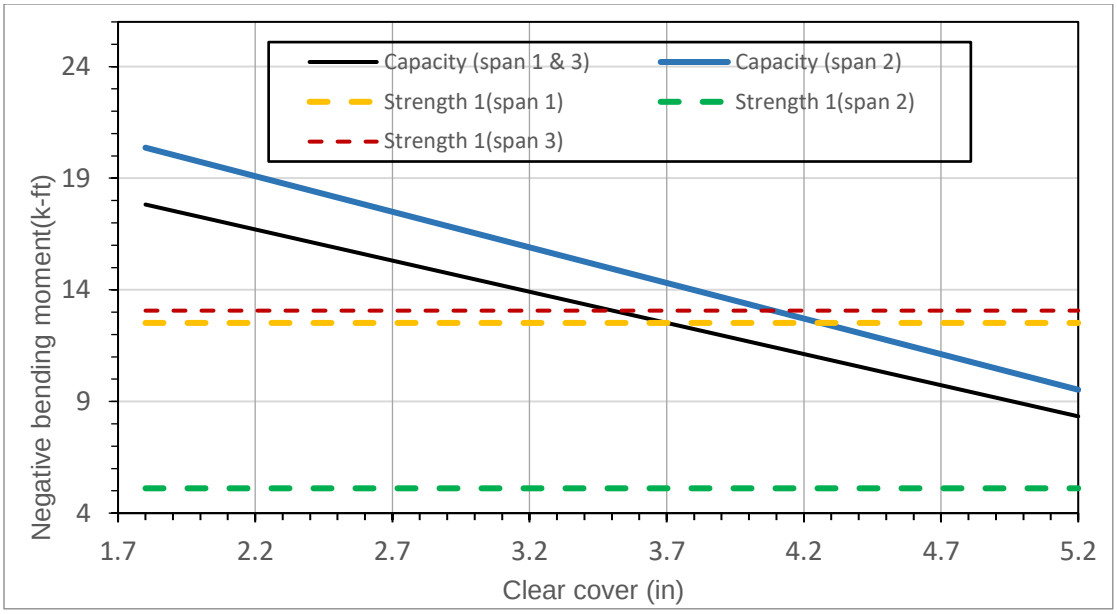

Figure 6-20 New SH183 over MacArthur Capacity vs design moment comparison

6.8 Old SH183 over MacArthur Eastbound

Due to stripping on asphalt layer on deck and presence on soil (Figure 6-21) the GPR scan shown huge variation of rebar cover. The Figure 6-22 shows the disturbance in radargram due to stripping of asphalt and presence of soil. Figure 6-23 shows the high cover at start and end of radargram, which is present in all radargram at start. This contributes to the high range of cover variation in old MacArthur bridge. The rebar cover range is from 1.5 to 7 in. (38 to 178mm), about 84.83 % lies with 2 to 4 in. (51 to 102mm) (Figure 6-24).

Figure 6-21 Presence of Soil on Deck

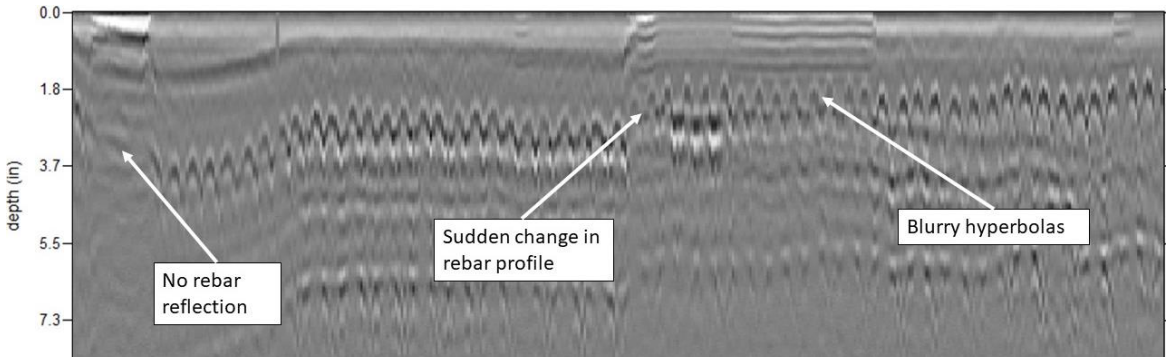

Figure 6-22 Radargram of old SH183 over MacArthur

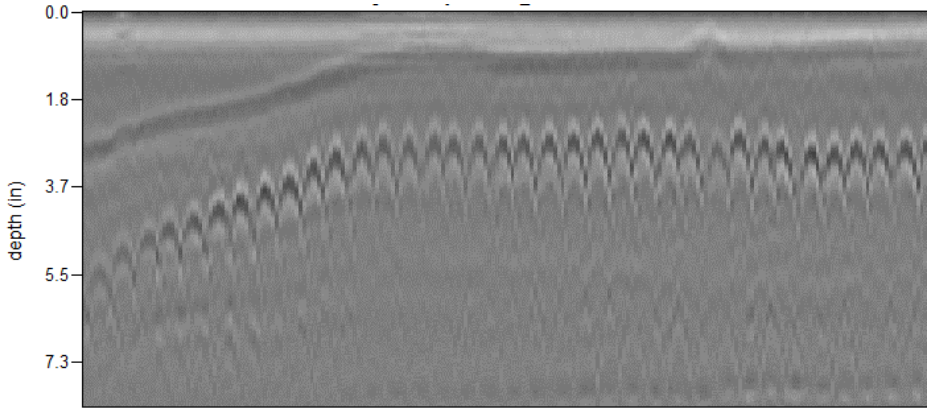

Figure 6-23 Sign of high cover at start of radargram

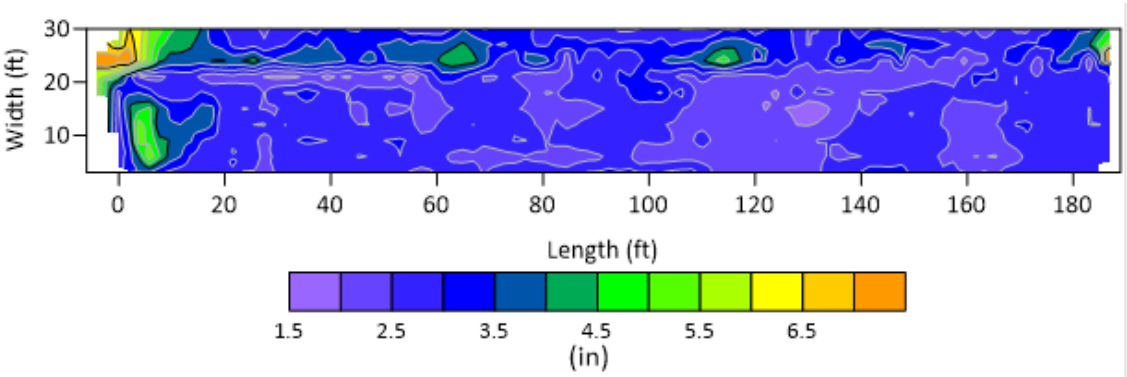

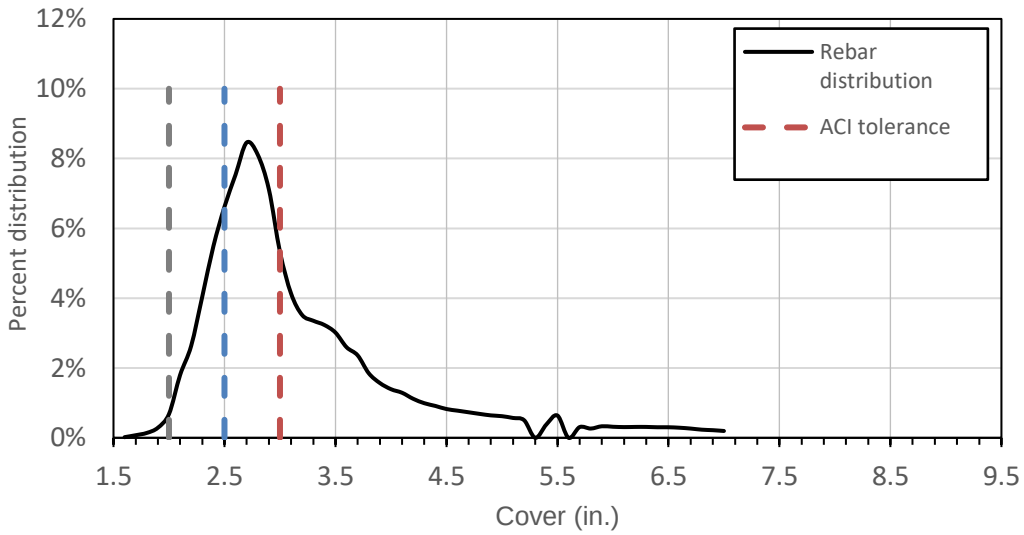

Figure 6-24 Old SH183 over MacArthur Eastbound Rebar Distribution

6.9 Old SH183 over MacArthur Westbound

Similarly, for 183 over MacArthur westbound high cover was observed at start and end on westbound of bridge (Figure 6-25). The rebar variation lies between 1.5 to 8 (38 to 203mm) inches, with 78.47% lies within 2 to 4 (51 to 101mm) inches (Figure 6-26). The Figure 6-27 is the design negative moment and capacity comparison.

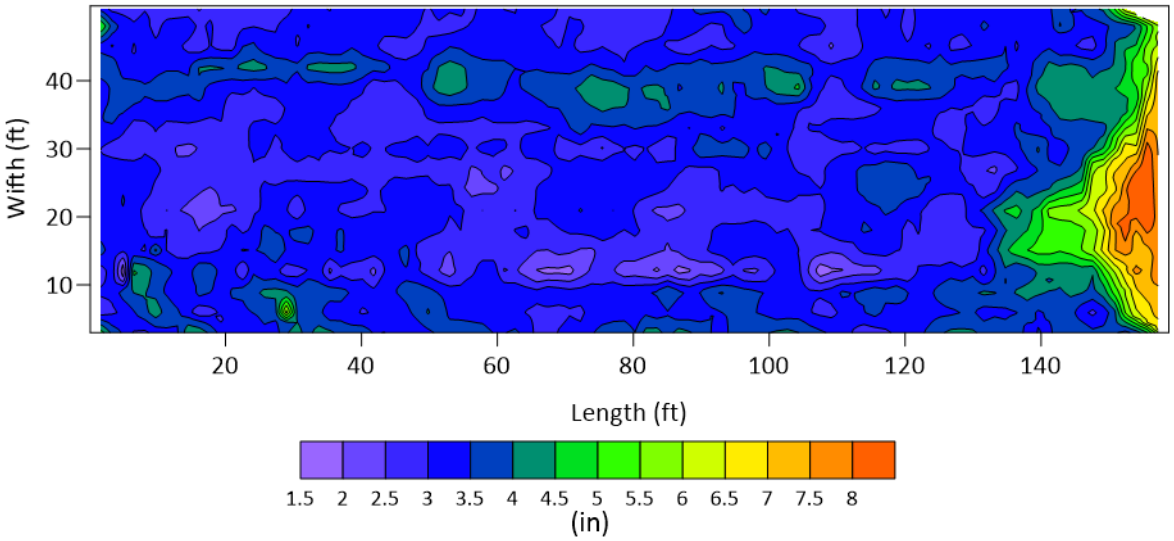

Figure 6-25 Old SH183 over MacArthur Westbound

The Table 6-5 is the standard deviation of the rebar distribution. Old SH183 over MacArthur shows large deviation while new bridges have less. This is due to change in dielectric constant which resulted in improper depth calculation.

Table 6-4 Standard deviation

Bridge			Standard deviation (in.)	Average (in.)
SH 183 over Loop	Old	Eastbound	0.48 (12mm)	2.15 (54mm)
		Westbound	0.36 (9mm)	2.25 (57mm)
	New	Eastbound	0.41 (10mm)	2.78 (71mm)
		Westbound	0.46 (12mm)	3.02 (77mm)
SH 183 over MacArthur	Old	Eastbound	0.95 (24mm)	3.21 (82mm)
		Westbound	1.2 (30mm)	3.74 (95mm)
	New	Eastbound	0.48 (12mm)	3.1 (79mm)
		Westbound	0.37 (9mm)	3.01 (77mm)

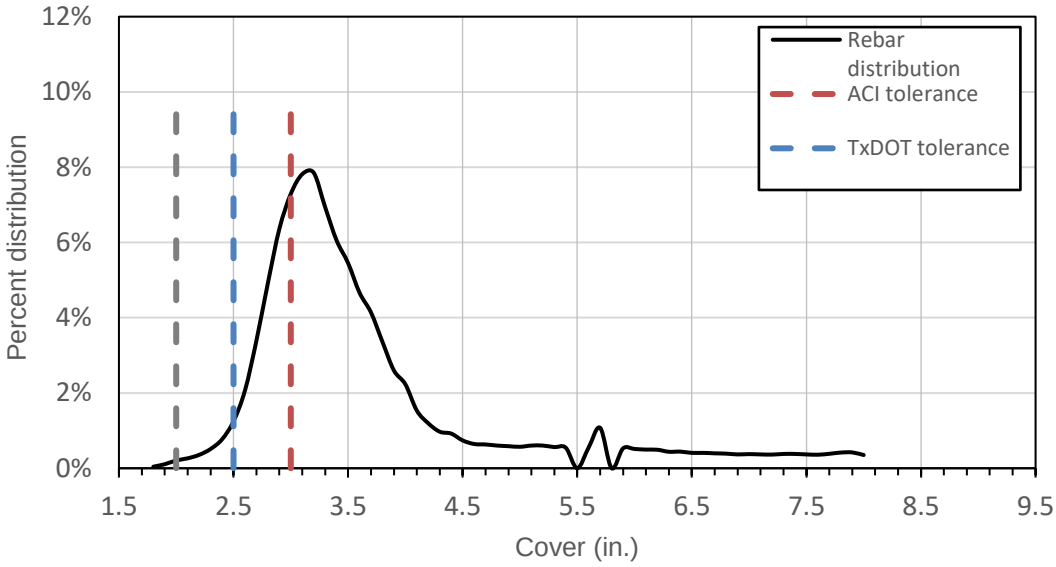

Figure 6-26 Old SH183 over MacArthur Westbound Rebar Distribution

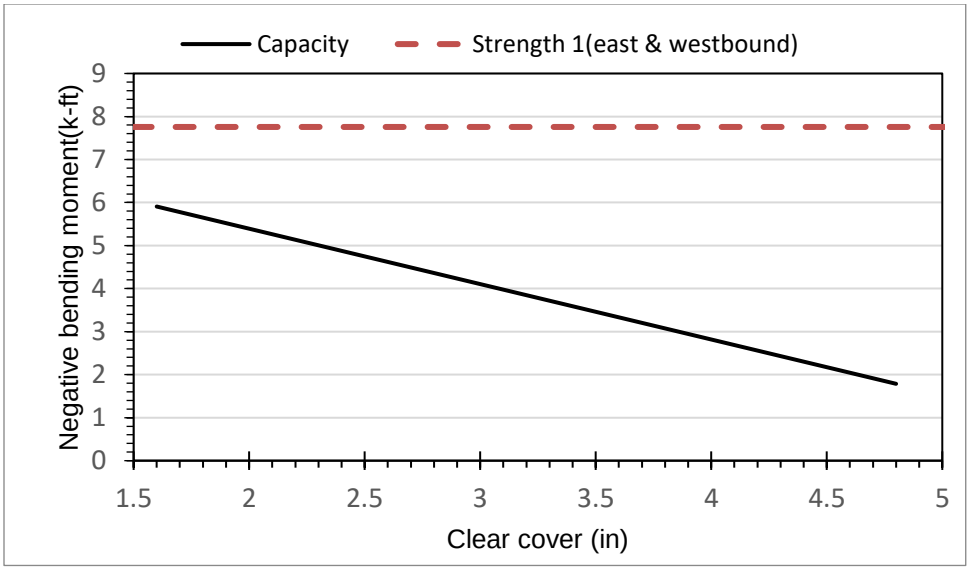

Figure 6-27 Negative bending moment vs clear cover for old SH183 over MacArthur

6.10 Deflection and Stresses on Rebar

One of the reasons for cover variation is the deflection of rebar due to a construction worker or heavy machinery placed on rebars. This section analyzes the deflection and stresses due to construction worker standing on rebar mesh and behavior of different sizes rebar. As per TxDOT Standard Specifications for Construction and Maintenance of Highways, Streets and Bridges gives suggestion to prevent displacement and keep reinforcement at proper distance from the formwork. The reinforcement is to be placed accurately in the forms and hold firmly in place before and during concrete placement by means of bar supports that are adequate in strength and number. It is recommended that individual bar support in rows at 4-ft (1.22m). maximum spacing in each direction. Place continuous type supports at 4-ft (1.22). maximum spacing.

The rebar cage was modeled and analyzed in RISA-3D. The load imposed by construction worker is 200 lb. (assumption for an average weight of construction worker)).

Since, the rebar is supported at 4-ft(1.22m) maximum spacing in both directions, the rebar cage is modeled within 4x4 ft boundary. The Figure 6-28 shows #5@6-in spacing modeled in RISA-3D with one force 200 lb. (890 N) at intersection of longitudinal and transverse rebars located close to center of rebar cage. However, this location may not be location that results in maximum deflection. The longitudinal rebar was assumed to be #5@9-in.

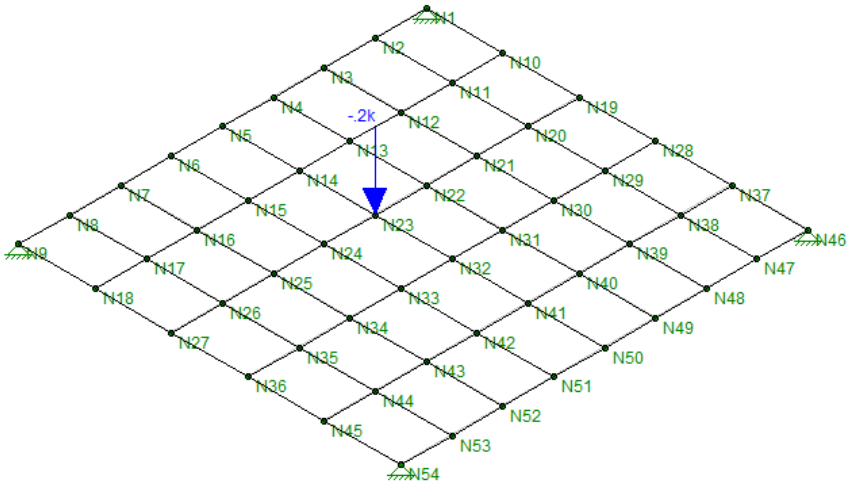

Figure 6-28 RISA-3D Model of Rebar Cage

The bar size and spacing were selected to achieve flexural resistance equivalent to deck with #5@6in, 2.5 in. (25.4mm) cover, slab thickness 8.5 in.(216mm), f'c= 4 ksi and fy= 60 ksi. Figure 6-29 is flexural resistance for different spacing and bar size. The bar spacing were rounded off to nearest whole number such that resistance is more than 14.6 k-ft (Table 6-5). The other parameters used for calculation of negative moment capacity is tabulated in Table 6-6.

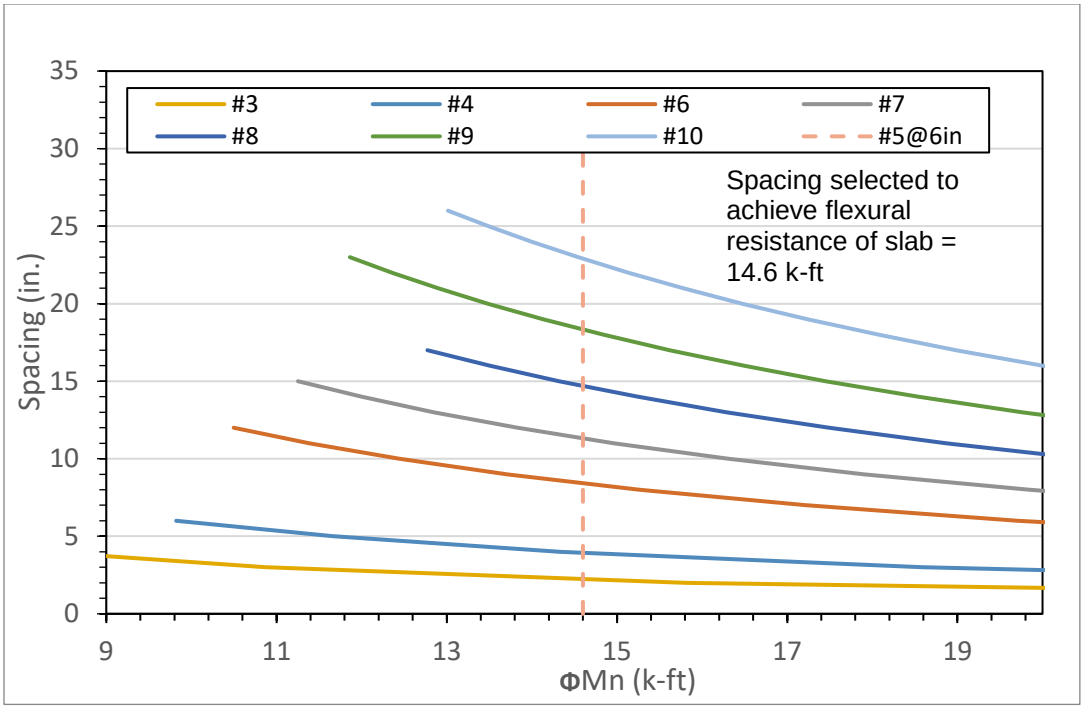

Figure 6-29 Selection criteria for spacing

Table 6-5 Transverse reinforcement negative moment capacity equivalent to capacity by #5@6-in.

Bar size @ spacing-in	**ΦM_n(k-ft)**
#3@2in	15.82 (109N/mm^2)
#4@3in	18.58 (128N/mm^2)
#5@6in	14.6 (101N/mm)
#6@8in	15.26 (105N/mm2)
#7@11in	14.97 (103N/mm2)
#8@14in	15.24 (105N/mm2)
#9@18in	14.84 (102N/mm2)
#10@22in	15.14 (104N/mm2)

Table 6-6 other parameters for negative moment calculations

f_y (ksi)	f_c (ksi)	Slab thickness (in.)	Top cover (in.)
60 (413.68 MPa)	4 (27.57 MPa)	8.5 (216 mm)	2.5(64 mm)

The actual mechanism between the rebar cage is complex. The modeling and analysis are based on following assumptions:

- The connection between the longitudinal and transverse rebar is fixed that is connecting ties does not deform.
- The transverse and longitudinal rebar does not provide support to each other and supports are only provided at each corner.
- Since, the rebar cage is continuous, and supports are provided at 4-ft (1.22mm) maximum spacing. Modeling is done only for single span supported by pin support; the rebar cage is continuous this represents severe condition. Continuous span will reduce the total deflection.

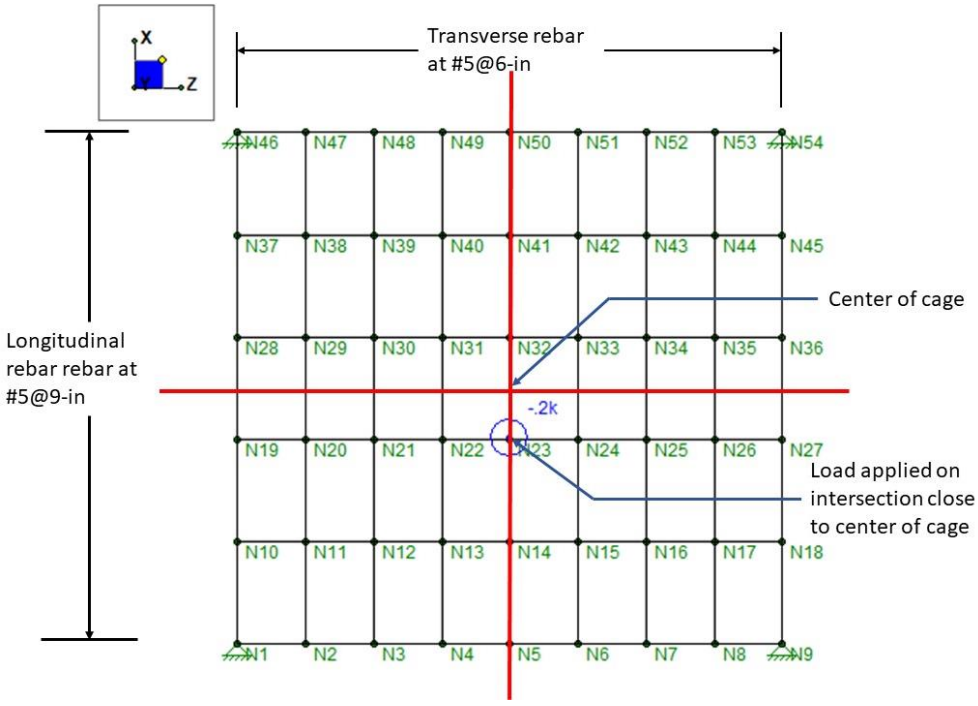

Figure 6-30 Typical Location of Applied Load

All the model with different bar sizes and spacing was analyzed and there maximum deflection and bending stresses is plotted in Figure 6-32 and Figure 6-31,

respectively. It can be observed from the graph that as the bar size decreases the bending stresses in the bar increses. For the bar size and spacing #3@2-in the bending stresses is more that the minimum yeild i.e 127 ksi. So, there will be some permanent deflection.

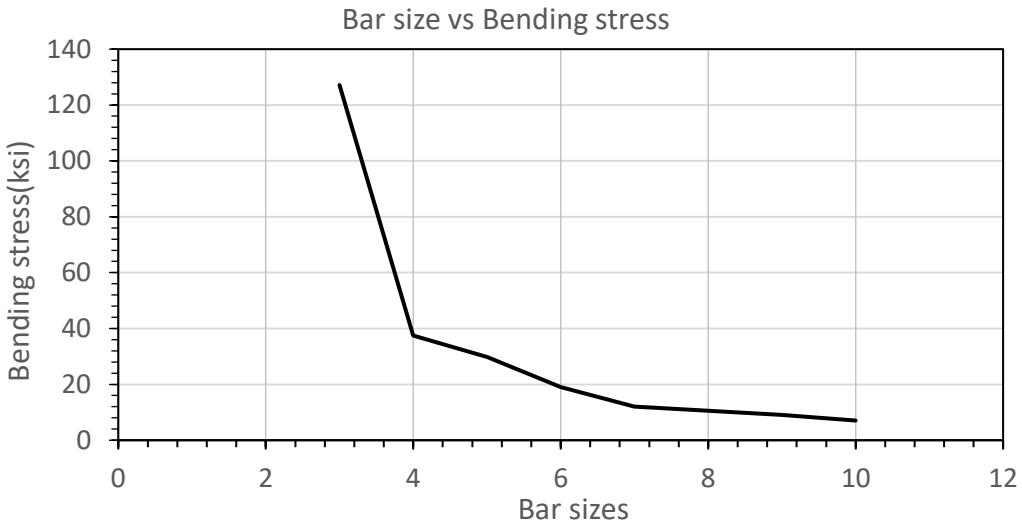

Figure 6-31 Bar Size vs Bending Stress

It can be observed from the Figure 6-32, the lower bar sizes deflects more than higher bar sizes and the deflection transition is expontial. The use of higher bar to reduce deflection will be advantageous. However, there may be more than one load acting on the rebar cage or the heavy machinery is placed on it. In that case the deflection will be more.

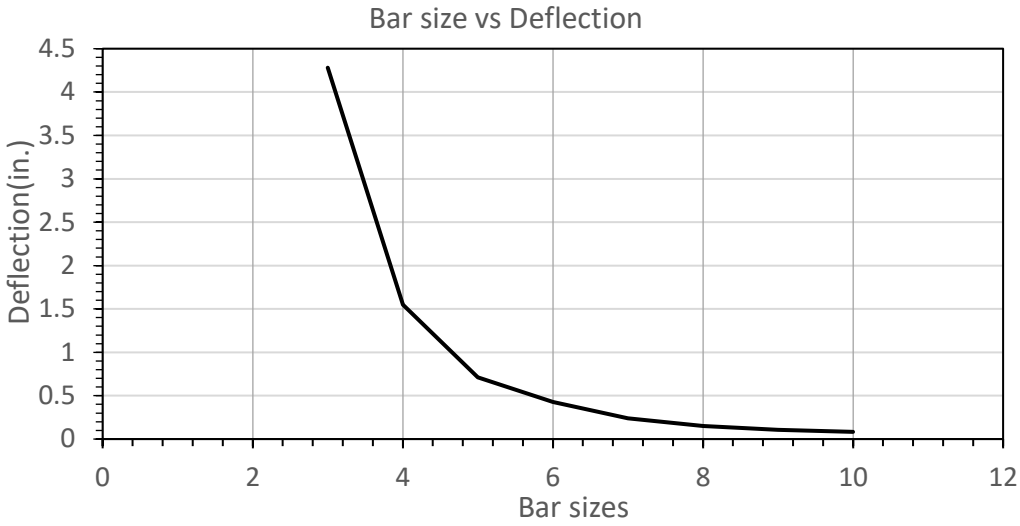

Figure 6-32 Bar Size vs Deflection

Generally, while construction of rebar cage, supports or spacers are missed due to improper inspection. This contributes to longer span and higher rebar cage deflection. To examine this RISA model for rebar cage supported longitudinally and transversely at 8 ft is modelled. Figure 6-33 and Figure 6-34 are modeled rebar cage with load applied as shown.

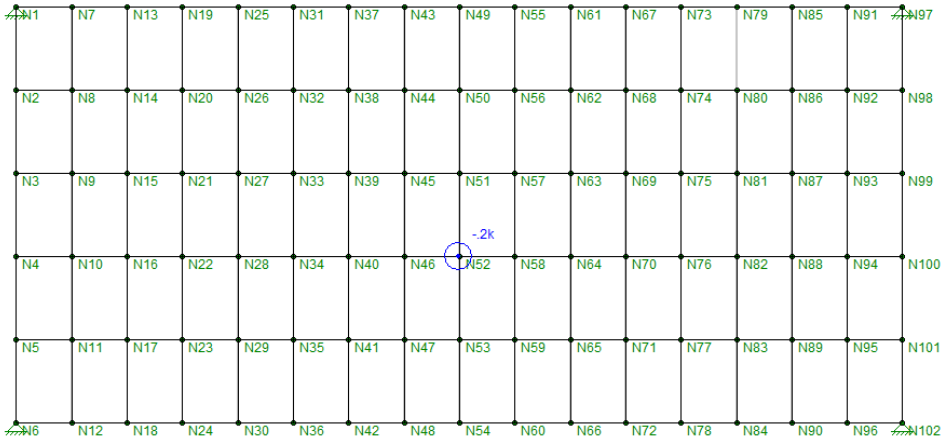

Figure 6-33: Transversely supported at 8 feet

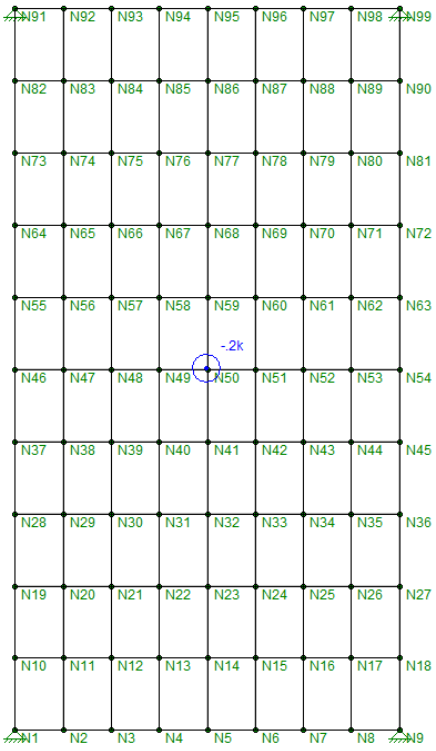

Figure 6-34 Longitudinally supported at 8 feet

Table 6-7 is the result of analysis. Longitudinally supported rebar cage will be deflected less about 3 in. (76mm) and stresses are within elastic range while rebar supported transversely deflects about 5 in. (127mm). with stresses exceeding yield.

Table 6-7 Result of missing support

Support	Max. Stress (ksi)	Max. Deflection (in)
Support spanning 8ft longitudinally	39.3 (271N/mm2	3.03 (77mm)
Support spanning 8-ft transversely	61.91 (427N/mm3	5.08 (129mm)

Since, analysis is done for model with 4 ft (1.22m) boundary, the single span will deflect more that multiple span. Now, 4 spans on each direction is tested to check deflection of rebar. The Figure 6-35 and Figure 6-36shows the analyzed model with loads on different position. This is for #5@6 in and #5 @ 9 in transverse and longitudinal spacing.

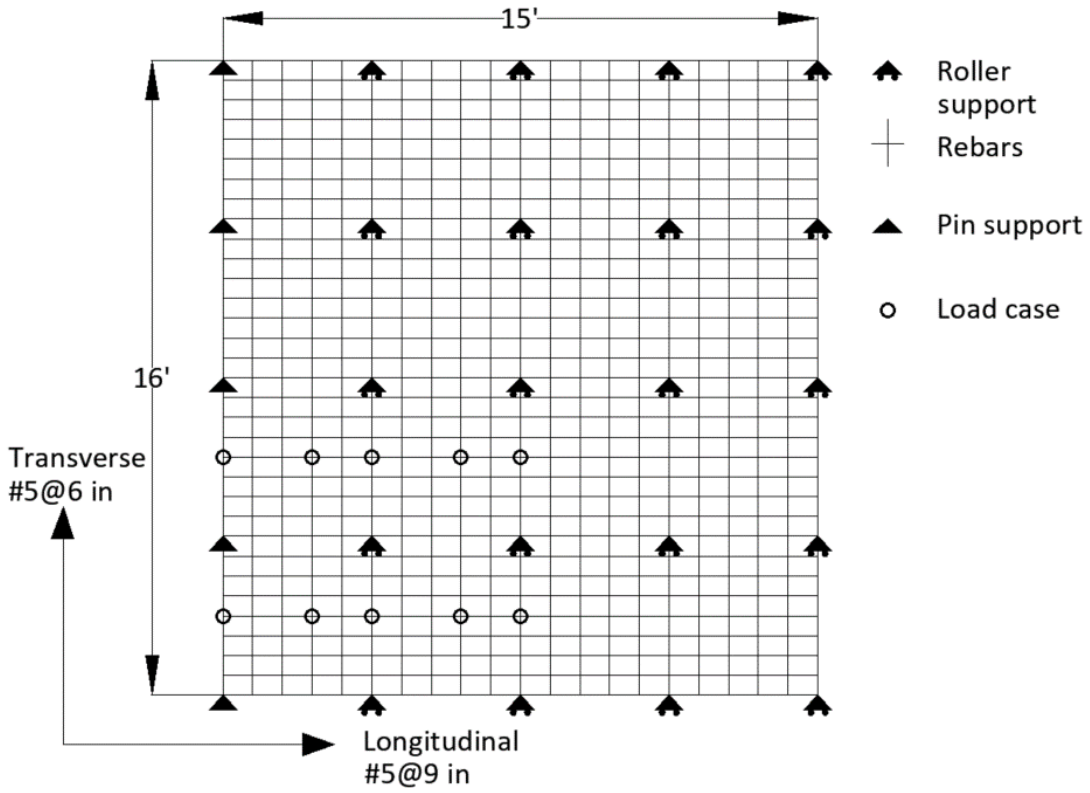

Figure 6-35 Continuous Rebar mat

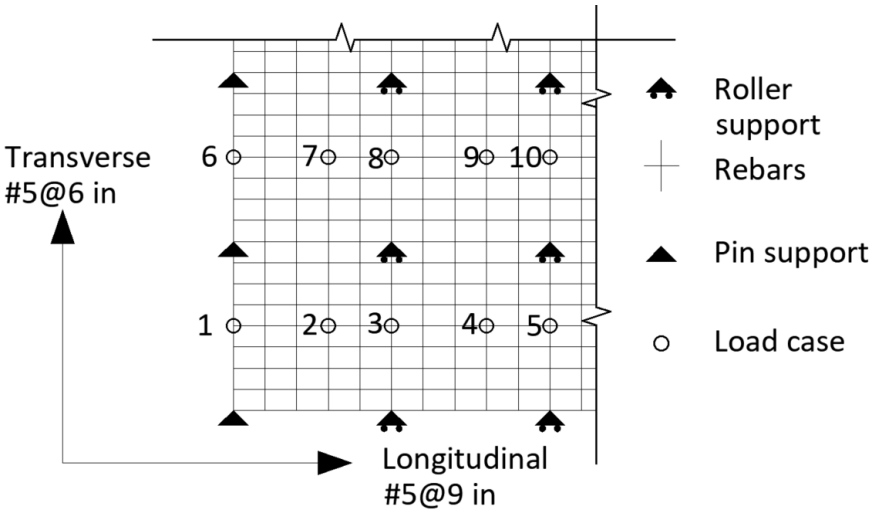

Figure 6-36 Applied load position

For single span the deflection is 0.711 in. (18mm). For continuous span rebar supports the deflection is less than one span rebar model (Table 6-8).

Table 6-8 Continuous Rebar Cage Results

Case	Stresses (ksi)	Deflection (in.)
1	37.08 (256 N/mm^2)	0.55 (14mm)
2	27.56 (190 N/mm^2)	0.4 (10mm)
3	28.24 (195 N/mm^2)	0.4 (10mm)
4	28.18 (194 N/mm^2)	0.4 (10mm)
5	27.44 (189 N/mm^2)	0.4 (10mm)
6	31.42 (217 N/mm^2)	0.37 (9mm)
7	26.32 (181 N/mm^2)	0.26 (7mm)
8	27.03 (186 N/mm^2)	0.26 (7mm)
9	27.27 (188 N/mm^2)	0.26 (7mm)
10	28.28 (195 N/mm^2)	0.26 (7mm)

Chapter 7

Conclusion and Future Research

7.1 Conclusion

In this chapter, summary of findings of the research and recommendation for future study is made in this chapter. In this study, two bridges about 58 years old at end for service life and two newly constructed were studied for cover variation. The data was collected with GPR, cover depths ware calculated with help of GPR-slice software and Surfer software was used to plot contours. Dielectric constant was accurately estimated with migration and compared with ground truth method. Due to increased cover the reduction in flexural resistance were determined and compared with required flexural resistance against negative moments. The following conclusion are made:

- It was found that for new bridges percent distribution of rebar for +1/2 inch (13mm) and +1 inch (25.4mm) was 29 to 50% and 71 to 86%, respectively. This also suggest rebar cover distribution satisfied ACI standards to a higher extent than TxDOT.
- For the old SH183 over Loop 12 the rebar depth was approximately determined which showed a peak at 2.3 in. (58mm) close to the proposed cover of 2 in. (51mm).
- Old SH183 over MacArthur showed high standard deviation in cover due to scanning on surface with wet soil and stripped asphalt layer. As a result, dielectric constant was varying horizontally throughout surface. Since, same dielectric constant was used throughout, that results in over or under estimation of cover in some areas on deck. In addition, cracks on deck will allow water to seep and will also change dielectric constant around it. This variability in dielectric constant is not taken into consideration.

- Since, the tolerance does not allow lowering of rebar from proposed cover very less about 17% and 5.05% of average rebar distribution was observed for New SH183 over loop 12 and MacArthur bridges.
- Since design moments and capacities are calculated with constant slab thickness, which cannot be true. Cause of slab variation can be due to uneven shrinkage of concrete and deflection in forms (except for stay-in-place forms).
- For new bridges, increase in rebar cover resulted in decrease in capacity, but not beyond the total factored design moment capacity of deck due to dead, wearing and live load. It can be concluded designing is done taking tolerance into consideration. For old bridges, calculated design moments in accordance to AASTHO 2017 resulted in higher design moments because older bridges were built with lower load factors and with HS20 loads.
- Modeling of rebar cage in RISA, resulted in higher rebar size deflect less and within elastic limit than lower sizes rebar deflects beyond elastic limit. Usage of #5 bars in slabs with cage supported 4 ft (1.22m) maximum spacing deflect within elastic limits.
- Rebars cage supported at an interval more than 4ft (1.22 m) resulted in higher deflection. There were differences in deflection of cage supported transversely and longitudinally

7.2 Future Work

- The concrete pouring on the deck is not always even this result in different thickness of slab. Using lower frequency antenna to estimate slab thickness and calculating capacity will be an accurate approach.

REFERENCES

1. American Concrete Institute (ACI).(2010). Specifications for Tolerances for Concrete Construction and Materials and Commentary, Detroit, Michigan.
2. American Association of State Highways and Transportation Officials (AASHTO). (2017). LRFD Bridge Design Specifications. Washington, DC: American Association of State Highways and Transportation Officials.
3. Istiaque Hasan, Md. (2015). Quantitative Non-Destructive Evaluation of Rebar Diameter and Corrosion Damage in Concrete Using Ground Penetrating Radar.
4. Istiaque Hasan, Md & Yazdani, Nur. (2016). Ground penetrating radar utilization in exploring inadequate concrete covers in a new bridge deck 104-114. 10.1155/2016/8536850.
5. Al-Qadi, I., & Lahouar, S. (2005). Part 4: Portland Cement Concrete Pavement: Measuring Rebar Cover Depth in Rigid Pavements with Ground-Penetrating Radar. Transportation Research Record: Journal of the Transportation Research Board, 1907, 80-85. doi:10.3141/1907-09
6. Parrillo, Robert ; Roberts, Roger. (1997). Ground Penetrating Radar for Highway and Bridge Deck Condition Assessment and Inventory. NDT & E International. 10.1016/s0963-8695(97)82182-2.
7. Texas Department of Transportation (TxDOT). (2014). Standard Specifications for Construction and Maintenance of Highways, Streets, and Bridges. Texas.
8. S Ekolu and F Solomon. (2015). Statistical Analysis of Concrete Cover in New Highway Bridges, IOP Conf. Ser.: Mater. Sci. Eng. 96 012081
9. Hugenschmidt J. (2002). Concrete bridge inspection with a mobile GPR system. Construct Build Mater 2002;16(200):147–54.

10. Geophysical Survey System, Incorporated (GSSI). (2001). RADAN7 user's guide, Nashua, New Hampshire 03060-3075 USA
11. Geophysical Archaeometry Laboratory Inc. GPR-Slice manual v7.0, 2018
12. Geophysical Survey System, Inc. (2011). SIR 30 Manual. Nashua, New Hampshire 03060-3075 USA
13. Geophysical Survey System, Inc. (2011). Concrete Handbook, Nashua, New Hampshire 03060-3075 USA
14. George C. Lee, Satish B, Mohan, Chao Huang, and Bastam N. Fard. (2013). A Study of U.S. Bridge Failures (1980-2012) (MCEER-13-0008). Buffalo, NY 14260.
15. Ibrahim Erdem and David B. Peraza. (2015). A Case Study on the Construction Defects of Reinforced Concrete Walls with Insulated Concrete Forms. Forensic Engineering 2015. 10.1061/9780784479711.052
16. https://maps.google.com/
17. A Nemetschek Company. RISA 3D. CA 92610
18. https://www.concreteconstruction.net/how-to/construction/placing-reinforcing-steel_o
19. Richard M. Barker Jay A. Puckett (2013). Design of Highway Bridges.

Biographical Information

Prem Egade is a student at The University of Texas at Arlington currently pursuing a Master of Science in Structural Engineering and Mechanics. He obtained his bachelor's degree in Civil Engineering from Mumbai University, India in 2015. He has worked as an intern at Larkins Realtors, India. He has done a project on prestressed post-tensioned (segmented) bridge girder and a case study on a prestressed bridge of New Mumbai Metro project. He has worked on inspection of bridge deck with Ground Penetrating Radar in determining rebar cover profile of bridges.